Scientific report: WR 96-07

KNMI

An ozone climatology based on ozonesonde measurements

J.P.F. Fortuin

De Bilt, 1996

Scientific report = wetenschappelijk rapport; WR 96-07

De Bilt, 1996

P.O. Box 201
3730 AE De Bilt
Wilhelminalaan 10
Telefoon 030-220 69 11
telefax 030-221 04 07

Auteur: J.P.F. Fortuin

UDC: 551.510.534
551.501.771
551.508.822
ISSN: 0169-1651
ISBN: 90-369-2112-0

© KNMI, De Bilt. Niets uit deze uitgave mag worden verveelvoudigd en/of openbaar gemaakt worden door middel van druk, fotocopie, microfilm, of op welke wijze dan ook, zonder voorafgaande schriftelijke toestemming van het KNMI.

An Ozone Climatology based on Ozonesonde Measurements

J.P.F. Fortuin

KNMI, P.O.Box 201, 3730 AE De Bilt, The Netherlands

November 1996

Contents

Chapter 1

Introduction

Because ozone influences the thermal structure of the atmosphere through both longwave and shortwave absorption, climate models need a realistic distribution of ozone to simulate climate correctly. However, to do this can be difficult, as ozone shows a high variability in both space and time. This is especially true in the troposphere where the residence time of ozone is short, hence tying its distribution to the local sources and sinks of ozone. Most crucial for climate simulations is the distribution of ozone near the tropopause, as the minimum temperatures encountered here contrast most with the Earth's surface temperature and allows for a maximal longwave forcing of the earth-troposphere system (cf. Fortuin et al. 1995). Satellite observations of ozone since around 1979 have allowed for the compilation of stratospheric ozone climatologies reaching down to about 20 km (e.g. the CIRA climatology, Keating et al., 1996), leaving however the crucial tropopause area out of reach. One way to solve this problem is by using prescribed ozone profiles, as is done for example in the GCM ECHAM4, where the altitude of maximum ozone concentration is prescribed as in Wilcox et al. (1977), assuming a total ozone distribution from London et al. (1976). Other solutions are to use the ozone fields calculated by chemistry transport models (CTM's), or, as is presented in this paper, use ozonesonde data to construct an ozone climatology.

A first attempt to construct an ozone climatology based entirely on observations was presented by Fortuin and Langematz (1994, hence called FL94). For the troposphere and lower stratosphere (surface-30hPa), the climatology used data from 33 ozonesonde stations scattered around the world, and matched it with the CIRA ozone climatology (70-0.003 hPa) described in Keating et al. (1996). This resulted in a zonal (17 zonal bands) and monthly mean ozone climatology prescribed at 34 pressure levels. A new version of the ozonesonde part (surface to 10 hPa, 12 levels) of this climatology is now presented, designed to improve some shortcomings of the previous one, to note:

- The FL94 climatology was compiled of ozonesonde data over different observation periods, spanning a range from 1966 to 1990. The policy was to try and match where possible the observation period of the ozonesonde stations with that of the CIRA climatology: 1978-1983. However, quite a number of stations ,especially in the Southern Hemisphere (SH), performed observations over entirely different

periods. The resulting climatology therefore included observations from before and after the onset of the Antarctic ozone hole, which is undesirable for climate simulations, especially in the SH. The current ozone climatology still copes with the problem of heterogeneous observation periods, but now focuses on a the period 1980-1991, which covers the ozone-hole era (but ends before the Pinatubo eruption) and also enables matching with an extended set of satellite ozone observations.

- The ozone profiles of individual stations need not be representative of the zonal mean, as was assumed in FL94. Especially at lower latitudes where the zonal belts are long, large longitudinal gradients in tropospheric ozone can exist, as can be seen for example from the total tropospheric ozone distribution between 50° N and 50° S, presented by Fishman et al. (1992). The total tropospheric ozone in their study is derived from subtracting two satellite datasets from each other: integrated stratospheric SAGE from TOMS total ozone, over the period 1979-1991 (cf. Fig. 3.1 in Chapter 3.1). In the ozone climatology presented here, this dataset by Fishman et al. (hence called the Fishman dataset) is used to scale the tropospheric ozone profiles of the individual stations to a zonal mean profile. At higher latitudes, the profiles of the stations were assumed representative of the zonal mean.

- After scaling the tropospheric ozone according to the Fishman data, the integral of the zonal mean ozone profiles was compared with the zonal mean TOMS data over the target period 1980-1991, and scaled accordingly. This was not done with the FL94 climatology.

- Unlike FL94, the current version also has an accompanying standard deviation climatology calculated from the same datasets and over the same period. For long reliable time series, this gives an indication of the natural variability, whereas for shorter time series it is more an indication of the reliability of the zonal mean ozone values.

- The current climatology incorporates a number of new ozonesonde stations (Reunion, Brazzaville, Ascension Island, Hilo, Samoa, Boulder and Alesund), whereas the datasets from other stations have been extended significantly with new observations (notably Natal and the South Pole). On the other hand, quite a number of stations used in the previous climatology have now been removed (Prague, Cagliari Elmas, Palestine, Trivandrum, Aspendale, Marambio, Mirrny, New Delhi, Garmish Partkirchen and Barrow), as they had either incompatible observation periods, or consisted of too few sonde releases to be of added value.

In the following, features of the ozonesonde stations that comprise the climatology will be discussed (chapter 2), followed by a description of the methods followed to compile the climatology (chapter 3) and a discussion (chapter 4).

Chapter 2

Ozonesonde Stations

The ozonesonde data from the various stations that constitute the climatology were obtained mostly from the World Ozone and Ultraviolet radiation Data Centre (WOUDC), but also through personal correspondence with the people mentioned in the Acknowledgements. If any of the station data presented here is used by other workers, the author requests that the associated sources as listed in the Acknowledgements are mentioned. Some of the station data have been analysed in previous studies, e.g., the Natal station data is discussed in a climatology study by Kirchoff et al. (1991), and the seasonal behaviour plus trends of most of the stations listed in Table 2.1 are presented in Logan (1985). The geographic location of the ozonesonde stations used in the climatology is shown in Fig. 2.1. Information on their observation periods and frequency, the instrument types used and the correction factor applied is given in Table 2.1.

Before incorporating the ozonesonde stations into the climatology, a primary inspection was performed by plotting the time series of various recorded parameters for each station, as is shown for a selection of 3 stations in Fig. 2.2. This was found to be a necessary control as for quite a few stations, revised time series were appended to the database without removing the outdated time series. Also, it provides a quick overview of the recording history and points out important issues like the regularity of the observations and possible changes in the instrument type. For example, Resolute station - like all the other Canadian stations - had a switch in instrument type (from Mast Brewer to ECC) at the end of the seventies, the effect of which can be clearly seen on the correction factor (CF) time series in Fig. 2.2. The correction factor is the ratio of the total ozone obervation over the integral of the recorded profile, and is generally accepted to give an indication of the quality of the recorded profile. A value close to unity indicates a good agreement between the two independent observations, and hence only a small adjustment in the profile recording. However, often the concurrent total ozone observations are not made, as can be seen for Hilo station (Fig. 2.2), from the early nineteen onward, in which case the correction value is set to a default unity. When plotting these parameters such a sequence of events becomes apparent and otherwise would have lead to a too optimistic CF-value if calculated directly from the database values. For quite a few stations, there are no concurrent total ozone

Table 2.1 Ozonesonde stations used in the climatology. Listed are the station number and name, annual surface pressure in hPa, latitude and longitude, the observation period and the number of sonde releases over this period, the instrument number (according to the WOUDC code standard: 1 = Brewer, type India; 10 = Mast Brewer, 16=Carbon Iodine, 19 = ECC(?), 99 = other, presumably ECC); and the correction factor (CF).

Station no. + name	P_{surf} (hPa)	Lat	Lon	Period	sondes	instr.	CF
018) Alert	1005	82.3	-62.2	87-92	331	331	1.00
089) Alesund	1008	78.9	11.9	90-92	231	19	-
024) Resolute	1007	74.4	-94.6	80-91	480	10,99	1.02
262) Sodankyla	986	67.3	26.4	89-92	258	99	1.02
077) Churchill	1011	58.5	-94.0	80-91	444	10,99	1.01
021) Edmonton	924	53.3	-113.3	80-91	433	10,99	1.03
076) Goose Bay	1008	53.2	-60.2	80-91	522	10,99	1.04
221) Legionowo	917	52.2	20.6	80-91	398	99	1.43
174) Lindenberg	898	52.1	14.1	80-91	904	99	1.21
099) Hohenpeissenberg	905	47.5	11.0	80-91	1590	10	1.09
156) Payerne	921	46.5	6.6	80-91	1399	10	1.15
197) Biscarosse	1012	44.2	-1.1	76-83	361	10	1.19
012) Sapporo	1012	43.0	141.2	78-93	151	16	1.03
067) Boulder	825	40.0	-105.2	80-91	330	99	1.00
107) Wallops Isl.	1018	37.6	-75.3	80-91	347	99	-
014) Tateno	1010	36.0	140.0	78-93	341	16	1.01
007) Kagoshima	983	31.4	130.4	78-93	151	16	1.01
109) Hilo	999	19.7	-155.1	82-92	372	99	1.05
187) Poona	949	18.3	73.5	70-86	186	1	1.27
329) Brazzaville	976	-4.0	15.0	90-92	69	19	-
219) Natal	1007	-5.5	-35.1	79-92	276	99	-
328) Ascension Isl.	1003	-7.6	-14.2	90-92	46	19	-
191) Samoa	1006	-14.2	-170.3	86-90	115	99	-
555) Reunion	999	-21.0	55.0	92-95	43	99	-
265) Irene	854	-25.2	28.1	90-93	118	99	1.08
254) Laverton	1013	-37.5	144.5	82-90	140	99,10	1.20
256) Lauder	969	-45.0	169.4	86-90	309	99	1.02
101) Syowa	985	-69.0	39.4	80-92	245	16	1.03
280) Forster	?	-70.5	11.5	85-91	399	99	1.13
111) South Pole	679	-90.0		86-92	419	99	1.01

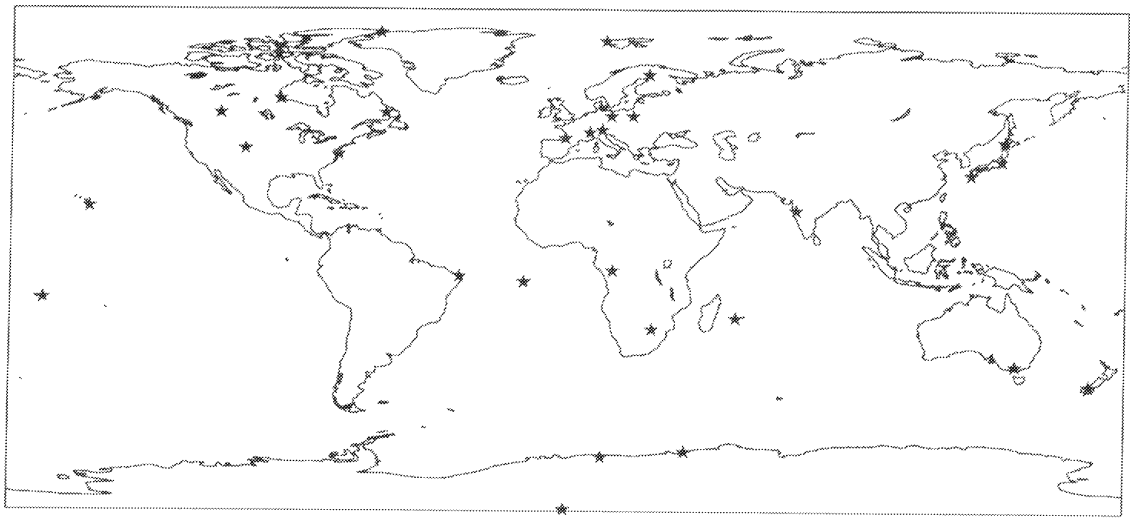

Figure 2.1 Geographical location of the ozonesonde stations (indicated as stars) used to compile the climatology

observations at all, which makes it impossible to assess the quality of the data (e.g., Alesund, Brazzaville, Natal, Ascension, Samoa and Reunion, see Table 2.1). For the South Pole, there is a long period in the seventies and eighties with no observations (cf. Fig. 2.2), until after the discovery of the ozone hole, when the programme was restarted again.

Whenever possible, data from the ozonesonde stations were selected over the target period 1980-1991, which covers the ozone hole period and excludes Pinatubo. However, for quite a few stations one had to settle for different periods, especially in remote areas where only limited observation intensives were performed (e.g., Brazzaville, Ascension, Reunion and Irene), or in the polar regions where concern for fast ozone depletion initiated observation programmes only later on in the eighties (e.g., Alert, Alesund, Sodankyla in the NH: Forster and South Pole in the SH). For the Japanese stations (Sapporo, Tateno and Kagoshima) a period extending 2 years on either side of the observation period was selected, due to the very limited amount of observations that would otherwise cover the summer months. Other stations with observations over different/shorter periods, but which were still included because of their strategic locations, are Biscarosse, Hilo, Laverton, and Lauder (cf. Table 2.1).

For each of the stations listed in Table 2.1, the monthly mean and standard deviation values over the observation periods were calculated. The resulting annual cycle

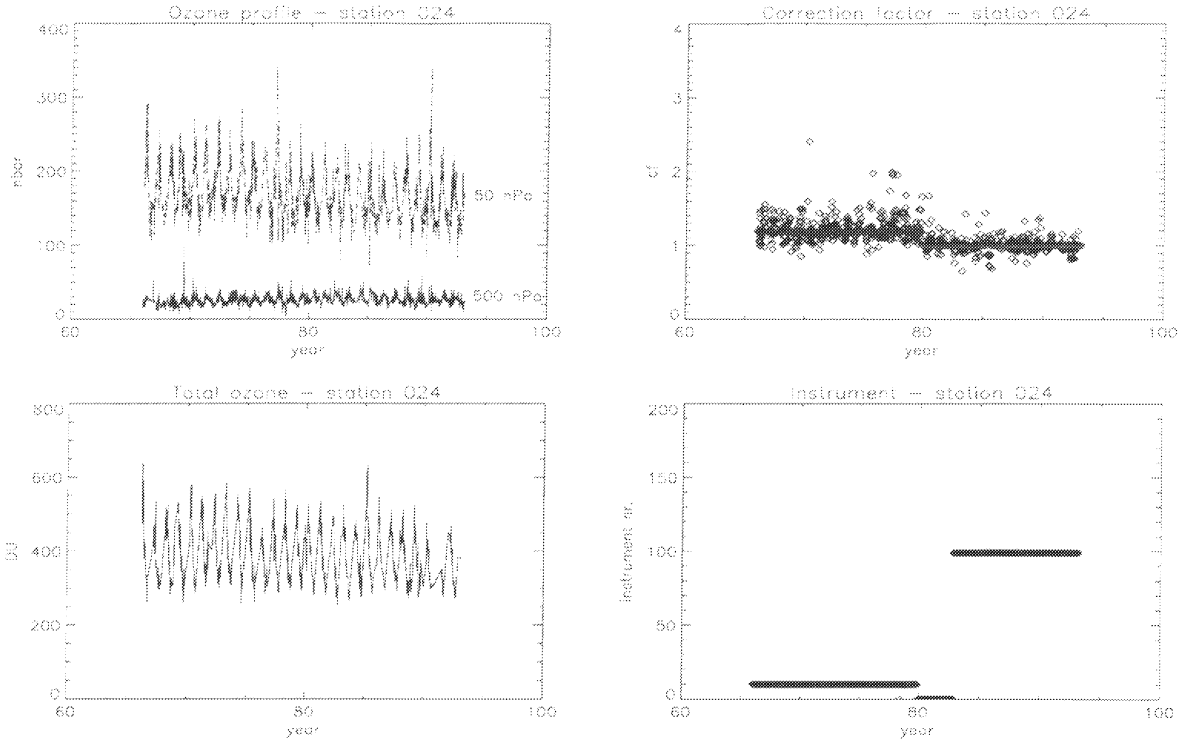

Figure 2.2 Time series of: ozone concentration at 500 and 50 hPa (in nbar, top left panel), total ozone (in DU, lower left panel), the correction factor (top right panel) and the ozonesonde instrument number (lower right panel, cf. Table 2.1 for corresponding instrument type); for Resolute station (above), Hilo station (next page, top 4 panels) and the South Pole (next page, bottom 4 panels).

for each station is shown in Fig. 2.3, plotted at the WOUDC standard pressure levels (1000, 700, 500, 300, 200, 150, 100, 70, 50, 30, 20, 10 hPa) against time. For two stations, Ascension and Reunion, too few sonde releases were available for respectively the month June and July, so the mean and standard deviation values for these months were obtained from linear interpolation between the neighbouring months. A couple of things to note in Fig 2.3, where the stations are depicted chronologically from North to South (similar to Table 2.1), are:

- In the Northern polar region, the early spring maximum concentration around 70 hPa is accompanied by a maximum standard deviation located just below it, around 100 hPa. This is not surprising, as the maximum variance can be expected somewhere between the altitude of highest concentrations and the altitude of highest dynamic variability: around the tropopause. It is important to note that the stations with more recent observation programmes, like Alesund (90-93) and Sodankyla (89-92), have lower spring maxima than the Canadian stations which recorded further back in time - especially for Resolute (80-91) and to a lesser extent Alert (87-92). Whether this an indication of accelerated

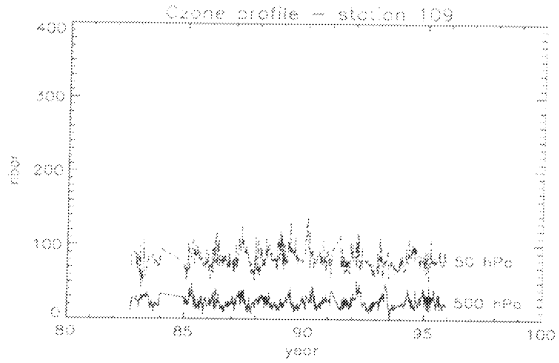
Ozone profile — station 109
ppbv
year
50 hPa
500 hPa

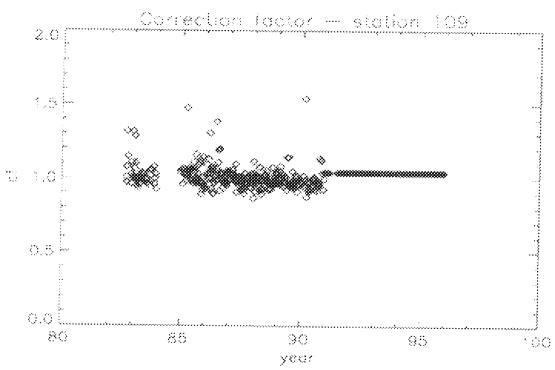
Correction factor — station 109
CF
year

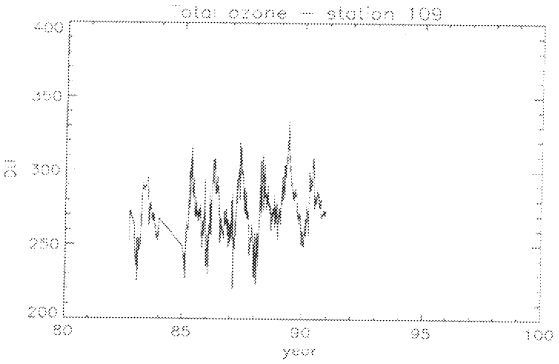
Total ozone — station 109
DU
year

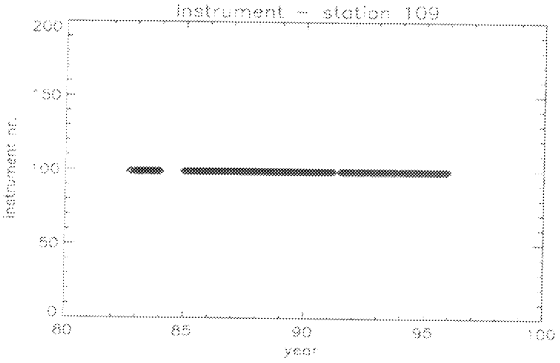
Instrument — station 109
Instrument nr.
year

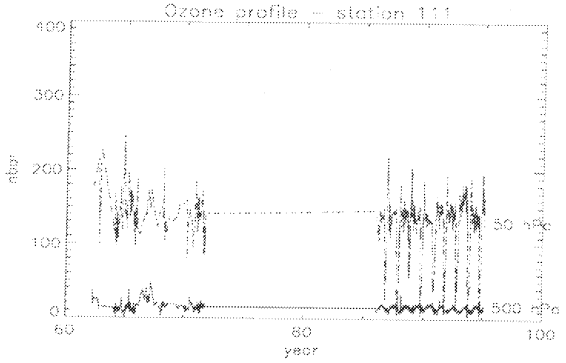
Ozone profile — station 111
ppbv
year
50 hPa
500 hPa

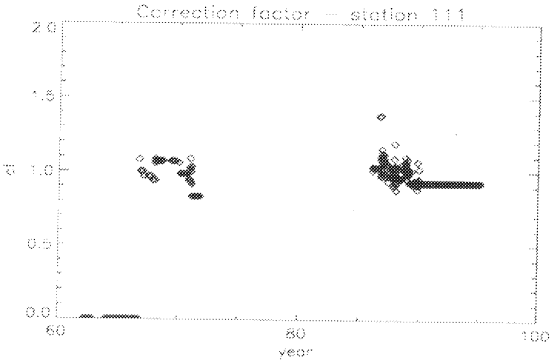
Correction factor — station 111
CF
year

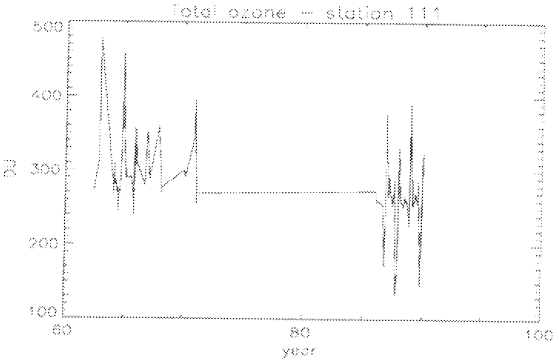
Total ozone — station 111
DU
year

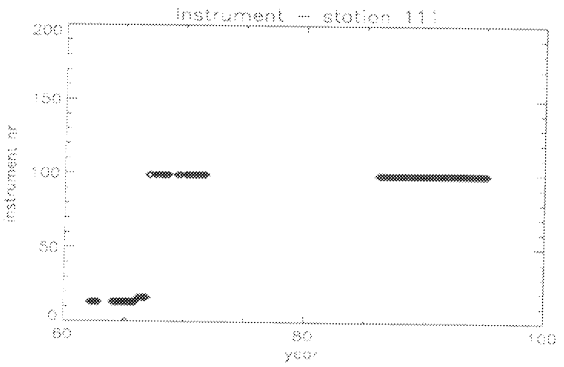
Instrument — station 111
Instrument nr.
year

stratospheric ozone depletion over the last years, or rather a spatial feature, is hard to say.

- The Northern midlatitudes has the best spatial coverage of ozonesonde stations, of which many have maintained a long and regular observation programme. Therefore, the observations here all cover about the same period (80-91) and can be readily compared with each other to point out spatial, rather than temporal, features in the ozone distribution. The spring maximum is now of comparable magnitude, but shows a latitudinal gradient with decreasing values toward lower latitudes. Again the maximum standard deviation is located beneath the maximum concentrations, but now moves back to early winter for the lower latitudes. Another evident spatial feature are the contrasts in tropospheric ozone, which for the more remote and pristine stations show a maximum in spring time (cf. Churchill, Edmonton, Boulder and Goose Bay in Canada), and for the stations in industrial regions show a summer maximum (Legionowo, Lindenberg, Hohenpeissenberg and Payerne in Europe). These maxima are probably associated with a high stratospheric influx during spring for the pristine regions versus photochemical smog during summer in the urban areas, as was also suggested by Logan (1985).

- Toward subtropical and lower latitudes in the NH, the seasonality in the mean ozone distribution becomes less pronounced whereas the tropopause and altitude of maximum ozone concentration shift steadily upward. The variance still has a pronounced maximum in the late winter which now seems to be located above and below the tropopause (e.g., Sapporo, Tateno, Kagoshima in Japan; Boulder and Wallops Island in the USA).

- Near the equator, hardly any seasonal variation in the tropopause height is discernible, whereas the maximum mean stratospheric concentration seems to coincide with the period of maximum solar insolation (e.g., Poona, Brazzaville, Natal, Ascension and Samoa). The stations Brazzaville and Ascension have so few sonde releases over the observation period that it is hard to infer whether the observed features here are coincidental or systematic - especially as far as the standard deviation is concerned. However, the high tropospheric ozone concentrations for these stations in the dry season is likely to be a systematic feature associated with biomass burning, as it also shows up in the longer record of Natal station. As is known from recent studies and observation campaigns on biomass burning (e.g., the SAFARI and TRACE-A campaigns, cf. Andreae et al., 1994) the associated ozone production - mostly confined to the SH - is widespread and comparable in magnitude to industrial smog pollution at NH midlatitudes (e.g., Andreae, 1994). This can also be illustrated with the Fishman dataset on tropospheric total ozone presented in Fig. 3.1 of the next chapter. It is note-

worthy that even on the remote island Samoa there is a discernable tropospheric ozone increase during this period. Whether this is a local feature or due to advection from a remote source region is hard to say. Further south, the island Reunion and the South African station Irene exhibit a similar temporary increase in tropospheric ozone, which could however also be associated with a maximal stratospheric influx in early spring, when the stratospheric variance reaches a maximum. A curious feature is the anticorrelation between tropospheric and stratospheric mean ozone at Irene station during September, along with anomalous high variances. The number of sondes over this month is similar to the neighbouring (quiet) months, which rules out a temporary anomaly. This seems to indicate some causal link between stratospheric and tropospheric ozone during this month which needs further attention.

- The few stations recording in the SH midlatitudes (Laverton in Australia and Lauder in New Zealand) indicate a similar seasonality in the mean ozone distribution as in the NH, with a spring maximum in the stratosphere. However, the corresponding standard deviation at a lower altitude is less pronounced and more shifted towards the winter season.

- In the SH polar region, all the stations (Syowa, Forster and South Pole) are located on the Antarctic continent, and therefore exhibit a clear ozone hole signal in the early spring. Similar to the NH polar stations, the stations have different observation periods that should be kept into account. Forster and South Pole observations go back to the mid-eighties, which may explain the deeper ozone hole compared to Syowa station where the record goes back to the early eighties. Different from the NH polar region, the maximum variability is now located at approximately the same altitude as (in stead of below) the average ozone maximum in the stratosphere, and seems to be associated with the occurrence of the ozone hole.

The ozone annual cycle could also have been presented in volume mixing ratio, in stead of nbar, for the above-mentioned stations. This would produce quite a different picture indicating especially the sources and sinks of ozone, rather than the dynamical features which can be inferred from the ozone partial pressure pictures. To illustrate this, the final ozone climatology (Chapter 4) will be presented in both partial pressure and volume mixing ratio units.

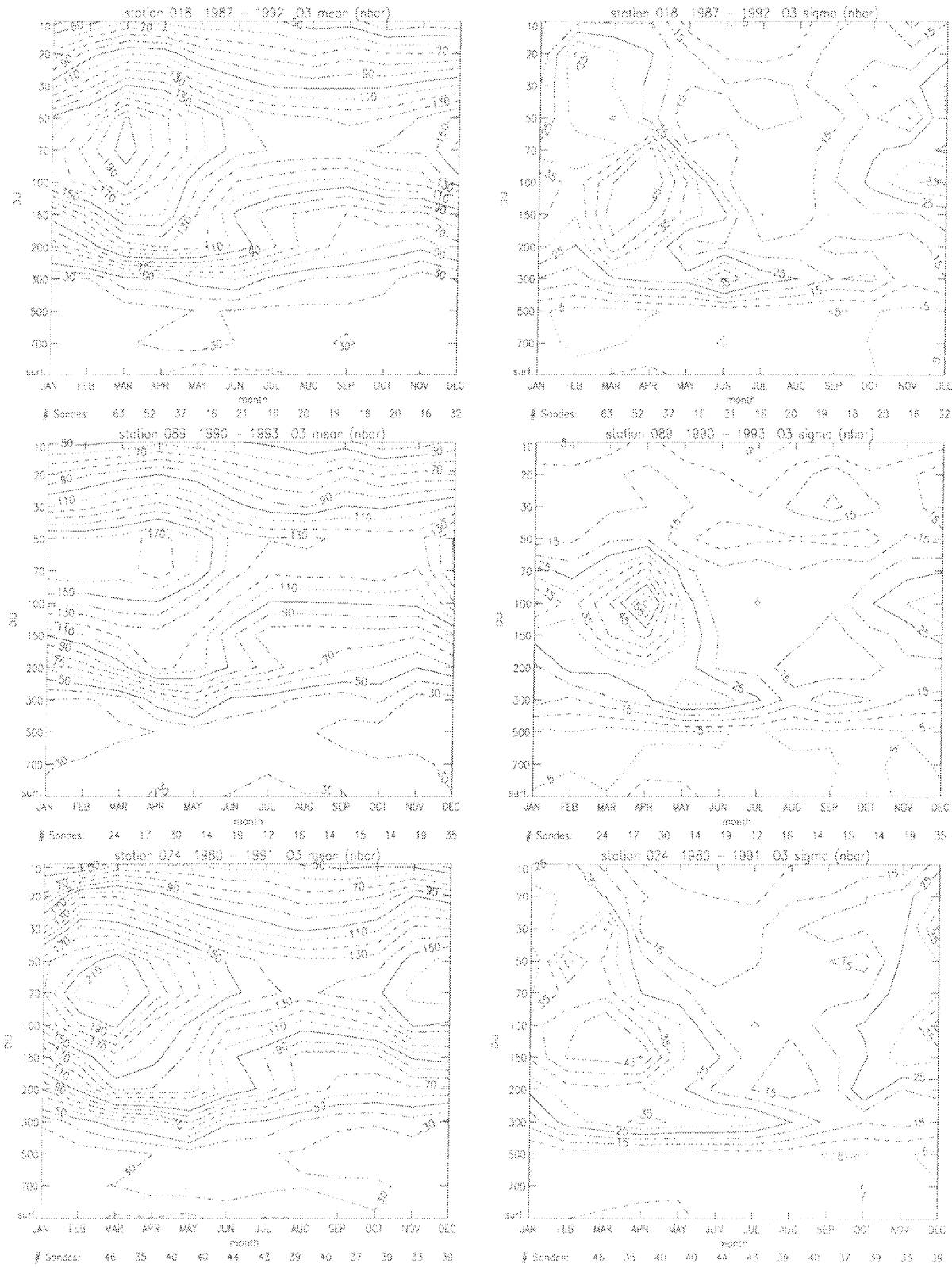

Figure 2.3 Above and following pages: For the ozonesonde stations listed in Table 2.1 (and in the same following order, i.e., from North to South), the annual cycle in the mean and standard deviation distribution of ozone - against the standard pressure levels at which the data is stored at the WOUDC.

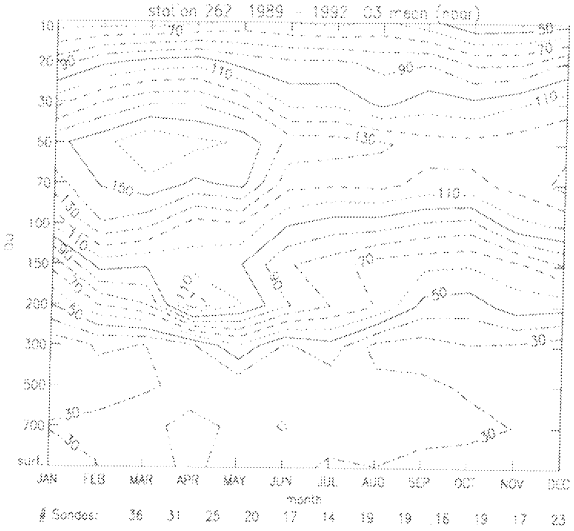
station 262 1989 – 1992 O3 mean (mbar)
DU
month
JAN FEB MAR APR MAY JUN JUL AUG SEP OCT NOV DEC
Sondes: 36 31 25 20 17 14 19 19 16 19 17 23

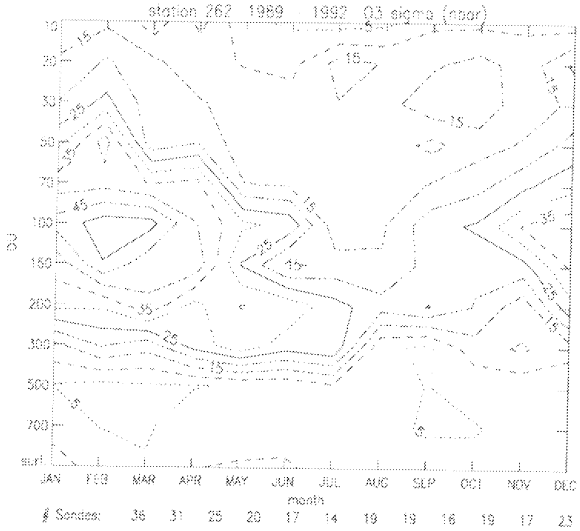
station 262 1989 – 1992 O3 sigma (mbar)
DU
month
JAN FEB MAR APR MAY JUN JUL AUG SEP OCT NOV DEC
Sondes: 36 31 25 20 17 14 19 19 16 19 17 23

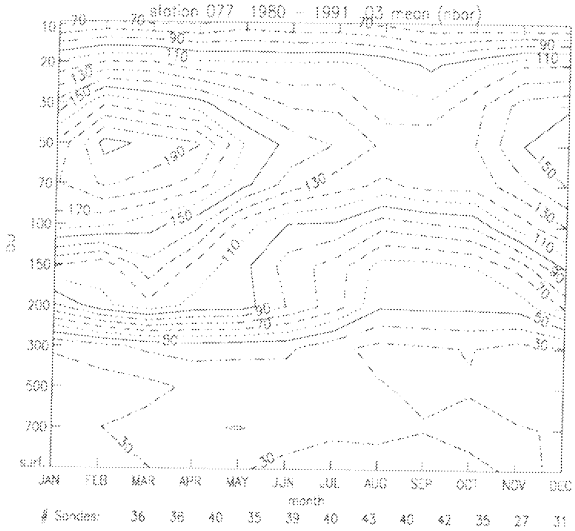
station 077 1980 – 1991 O3 mean (mbar)
DU
month
JAN FEB MAR APR MAY JUN JUL AUG SEP OCT NOV DEC
Sondes: 36 36 40 35 39 40 43 40 42 35 27 31

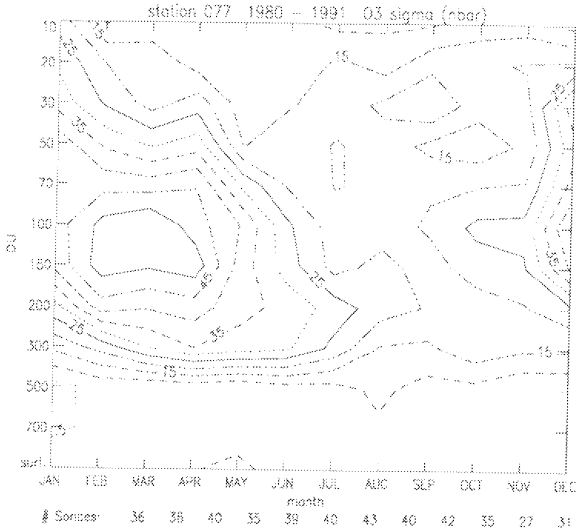
station 077 1980 – 1991 O3 sigma (mbar)
DU
month
JAN FEB MAR APR MAY JUN JUL AUG SEP OCT NOV DEC
Sondes: 36 36 40 35 39 40 43 40 42 35 27 31

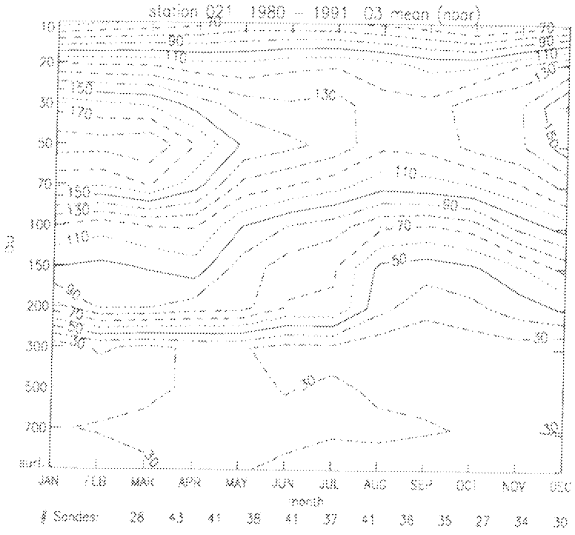
station 021 1980 – 1991 O3 mean (mbar)
DU
month
JAN FEB MAR APR MAY JUN JUL AUG SEP OCT NOV DEC
Sondes: 28 43 41 38 41 37 41 36 35 27 34 30

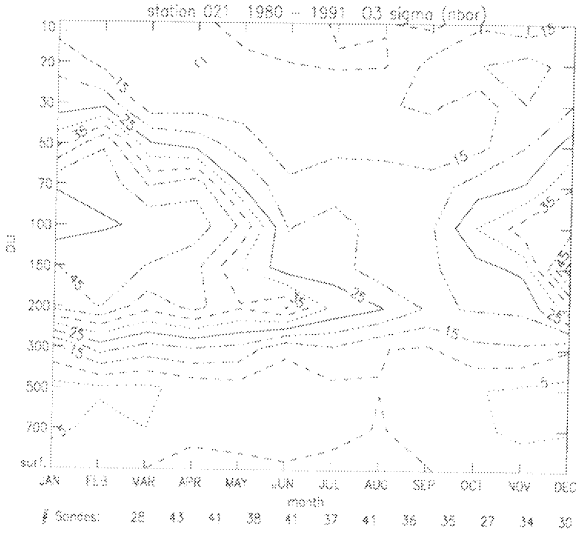
station 021 1980 – 1991 O3 sigma (mbar)
DU
month
JAN FEB MAR APR MAY JUN JUL AUG SEP OCT NOV DEC
Sondes: 28 43 41 38 41 37 41 36 35 27 34 30

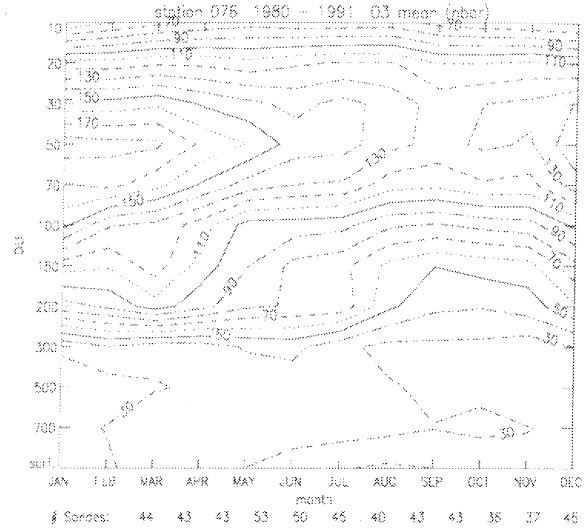
station 076 1980 – 1991 O3 mean (nbar)
DU
month
JAN FEB MAR APR MAY JUN JUL AUG SEP OCT NOV DEC
Sondes: 44 43 43 53 50 45 40 43 43 36 37 45

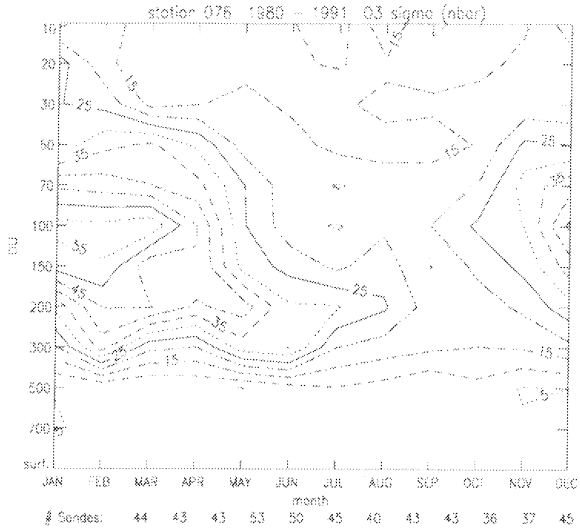
station 076 1980 – 1991 O3 sigma (nbar)
DU
month
JAN FEB MAR APR MAY JUN JUL AUG SEP OCT NOV DEC
Sondes: 44 43 43 53 50 45 40 43 43 36 37 45

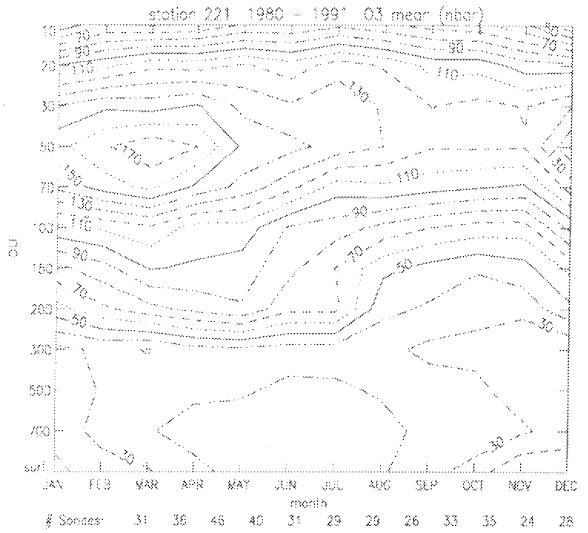
station 221 1980 – 1991 O3 mean (nbar)
DU
month
JAN FEB MAR APR MAY JUN JUL AUG SEP OCT NOV DEC
Sondes: 31 36 46 40 31 29 29 26 33 35 24 28

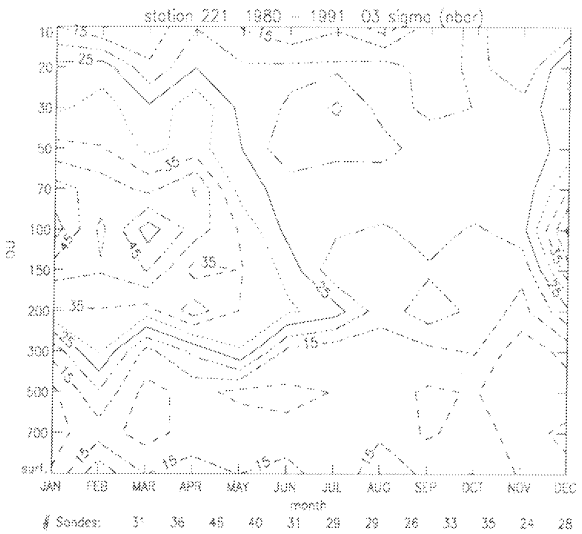
station 221 1980 – 1991 O3 sigma (nbar)
DU
month
JAN FEB MAR APR MAY JUN JUL AUG SEP OCT NOV DEC
Sondes: 31 36 46 40 31 29 29 26 33 35 24 28

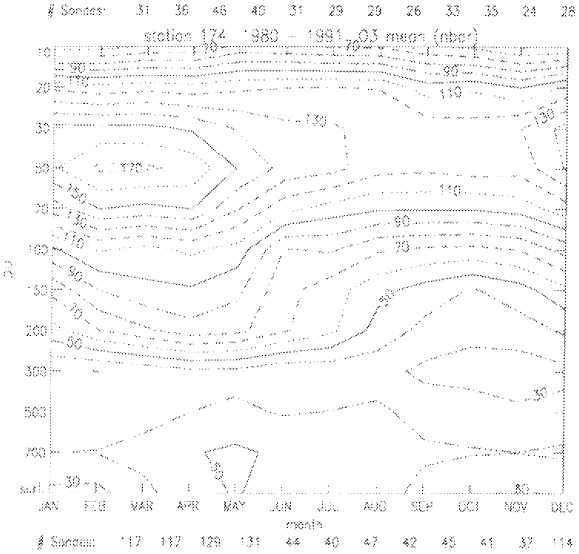
station 174 1980 – 1991 O3 mean (nbar)
DU
month
JAN FEB MAR APR MAY JUN JUL AUG SEP OCT NOV DEC
Sondes: 117 117 129 131 44 40 47 42 45 41 37 114

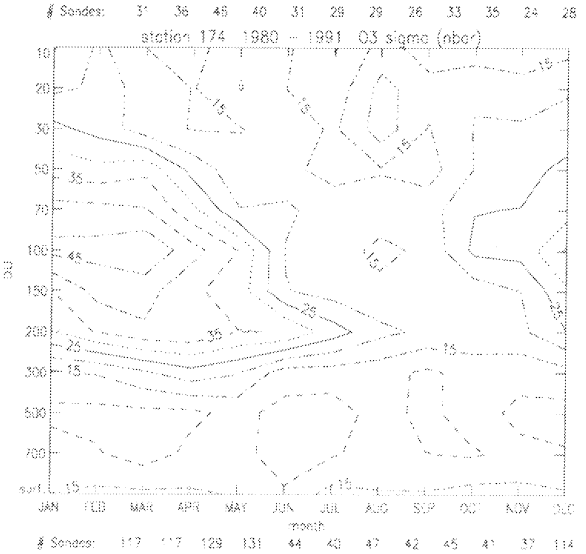
station 174 1980 – 1991 O3 sigma (nbar)
DU
month
JAN FEB MAR APR MAY JUN JUL AUG SEP OCT NOV DEC
Sondes: 117 117 129 131 44 40 47 42 45 41 37 114

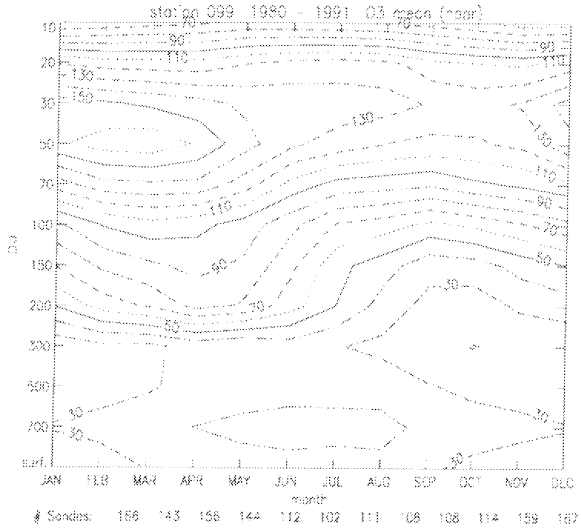
station 099 1980 - 1991 O3 mean (mbar)
DU
month
JAN FEB MAR APR MAY JUN JUL AUG SEP OCT NOV DEC
Sondes: 166 143 156 144 112 102 111 108 108 114 159 167

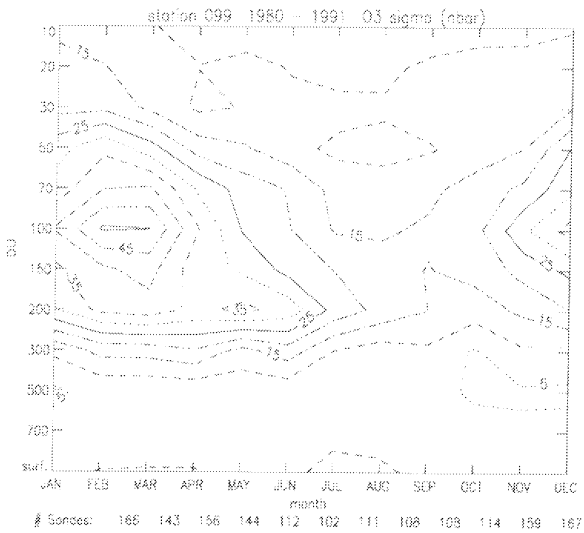
station 099 1980 - 1991 O3 sigma (mbar)
DU
month
JAN FEB MAR APR MAY JUN JUL AUG SEP OCT NOV DEC
Sondes: 166 143 156 144 112 102 111 108 108 114 159 167

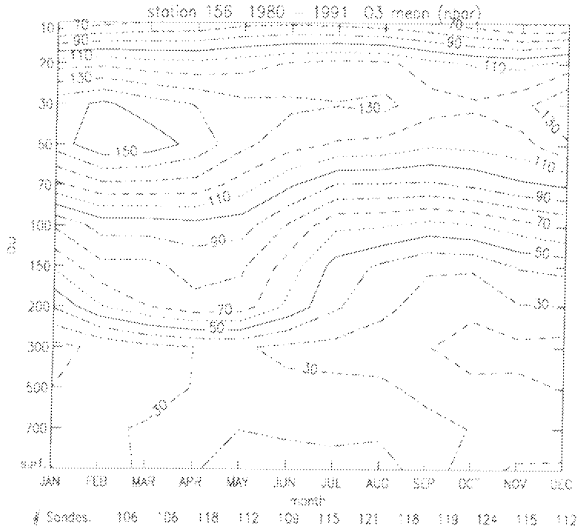
station 156 1980 - 1991 O3 mean (mbar)
DU
month
JAN FEB MAR APR MAY JUN JUL AUG SEP OCT NOV DEC
Sondes: 106 106 118 112 109 115 121 118 119 124 115 112

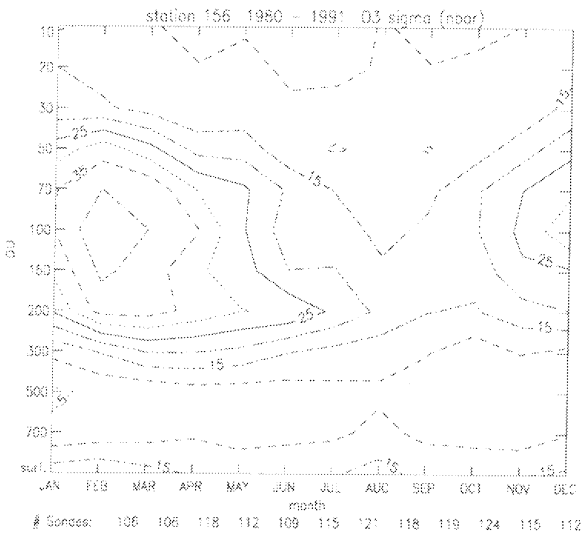
station 156 1980 - 1991 O3 sigma (mbar)
DU
month
JAN FEB MAR APR MAY JUN JUL AUG SEP OCT NOV DEC
Sondes: 106 106 118 112 109 115 121 118 119 124 115 112

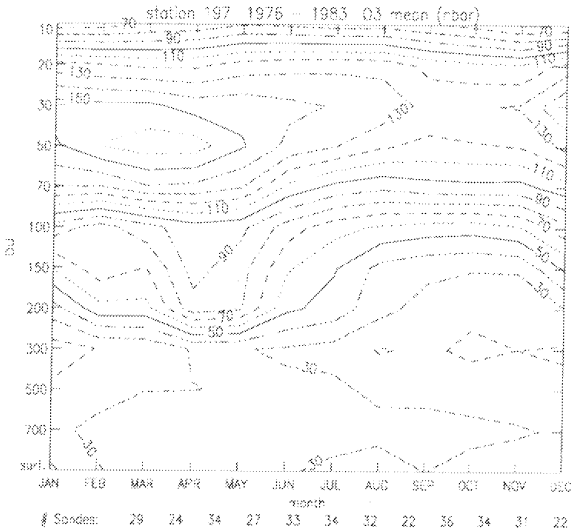
station 197 1976 - 1983 O3 mean (mbar)
DU
month
JAN FEB MAR APR MAY JUN JUL AUG SEP OCT NOV DEC
Sondes: 29 24 34 27 33 34 32 22 36 34 31 22

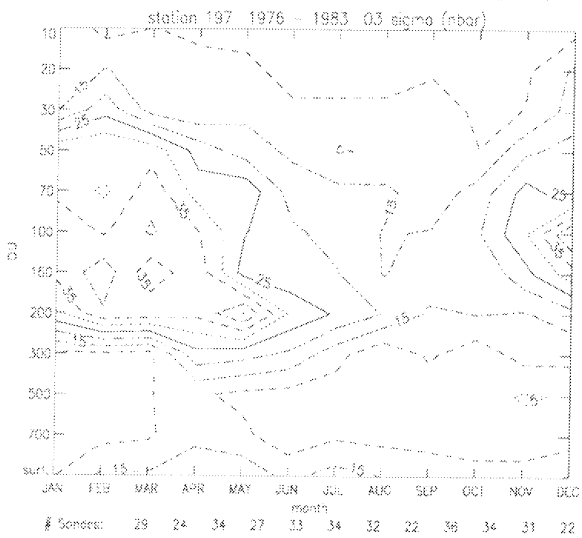
station 197 1976 - 1983 O3 sigma (mbar)
DU
month
JAN FEB MAR APR MAY JUN JUL AUG SEP OCT NOV DEC
Sondes: 29 24 34 27 33 34 32 22 36 34 31 22

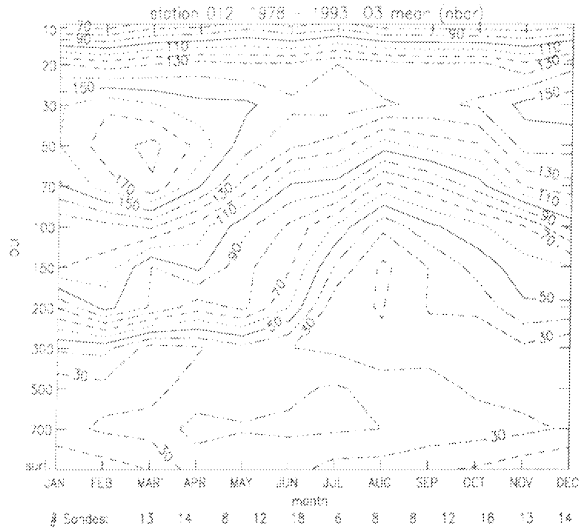
station 012 1978 - 1993 O3 mean (mbar)
DU
month
JAN FEB MAR APR MAY JUN JUL AUG SEP OCT NOV DEC
Sondes: 13 14 8 12 18 6 8 8 12 18 13 14

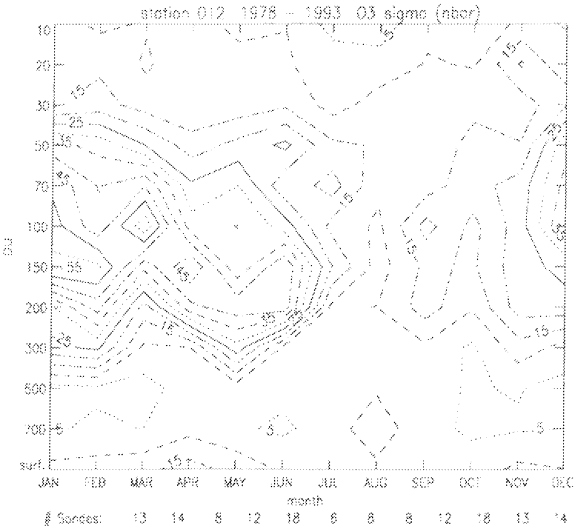
station 012 1978 - 1993 O3 sigma (mbar)
DU
month
JAN FEB MAR APR MAY JUN JUL AUG SEP OCT NOV DEC
Sondes: 13 14 8 12 18 6 8 8 12 18 13 14

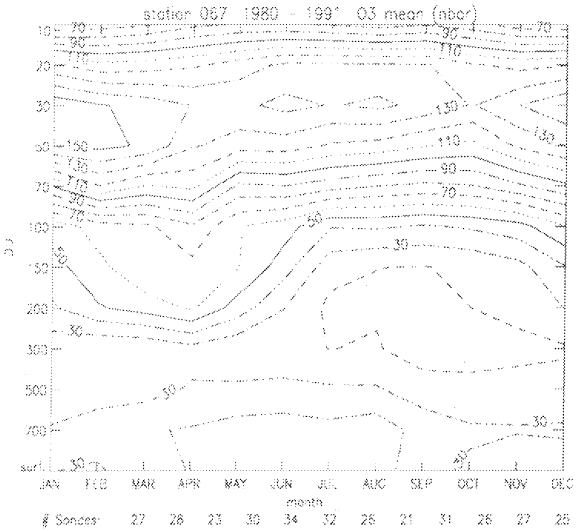
station 067 1980 - 1991 O3 mean (mbar)
DU
month
JAN FEB MAR APR MAY JUN JUL AUG SEP OCT NOV DEC
Sondes: 27 28 23 30 34 32 26 21 31 26 27 25

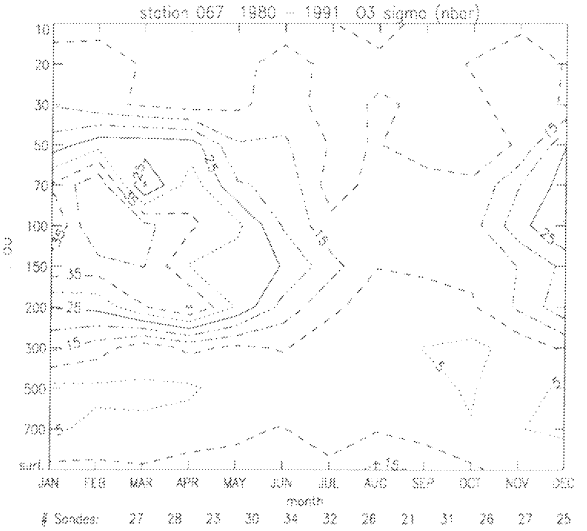
station 067 1980 - 1991 O3 sigma (mbar)
DU
month
JAN FEB MAR APR MAY JUN JUL AUG SEP OCT NOV DEC
Sondes: 27 28 23 30 34 32 26 21 31 26 27 25

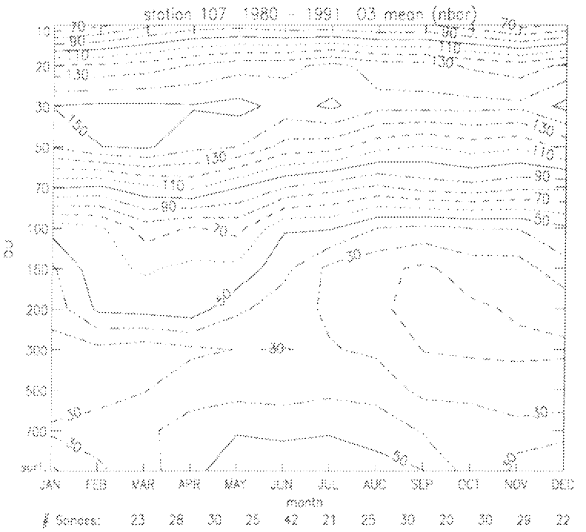
station 107 1980 - 1991 O3 mean (mbar)
DU
month
JAN FEB MAR APR MAY JUN JUL AUG SEP OCT NOV DEC
Sondes: 23 28 30 25 42 21 25 30 20 30 29 22

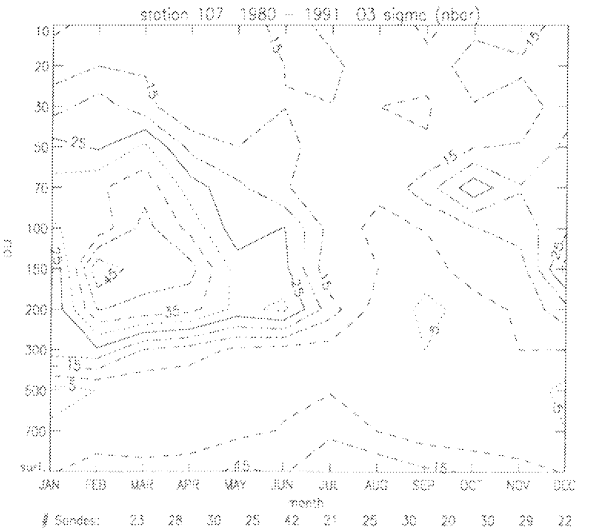
station 107 1980 - 1991 O3 sigma (mbar)
DU
month
JAN FEB MAR APR MAY JUN JUL AUG SEP OCT NOV DEC
Sondes: 23 28 30 25 42 21 25 30 20 30 29 22

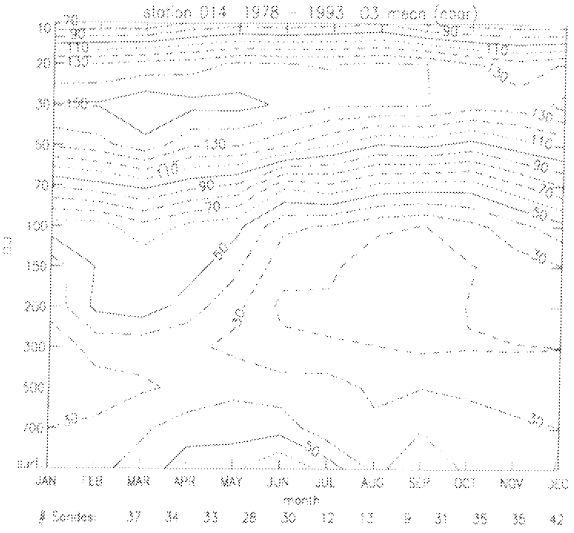
station 014 1978 - 1993 O3 mean (nbar)
DU
month
JAN FEB MAR APR MAY JUN JUL AUG SEP OCT NOV DEC
Sondes: 37 34 33 28 30 12 13 9 31 35 35 42

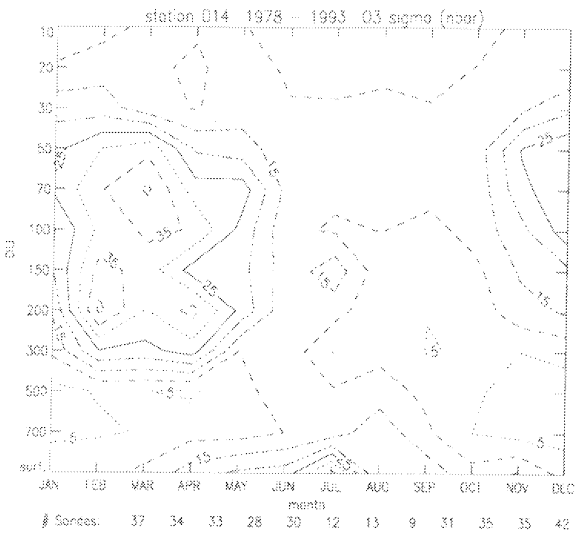
station 014 1978 - 1993 O3 sigma (nbar)
DU
month
JAN FEB MAR APR MAY JUN JUL AUG SEP OCT NOV DEC
Sondes: 37 34 33 28 30 12 13 9 31 35 35 42

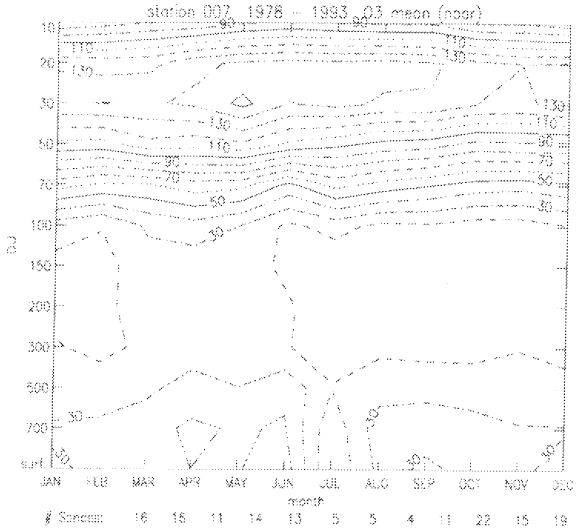
station 007 1978 - 1993 O3 mean (nbar)
DU
month
JAN FEB MAR APR MAY JUN JUL AUG SEP OCT NOV DEC
Sondes: 16 16 11 14 13 5 5 4 11 22 15 19

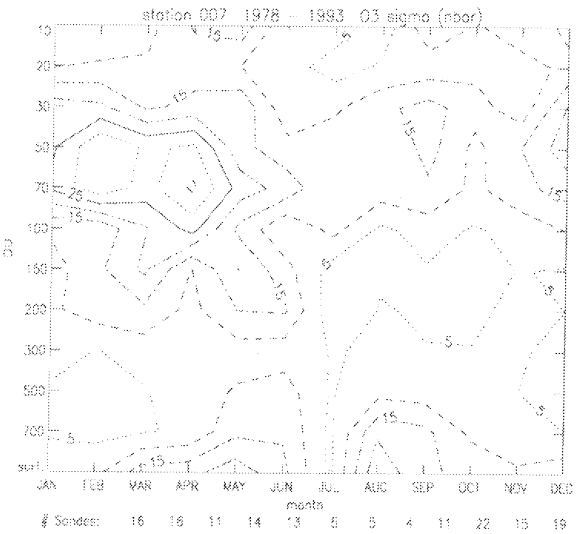
station 007 1978 - 1993 O3 sigma (nbar)
DU
month
JAN FEB MAR APR MAY JUN JUL AUG SEP OCT NOV DEC
Sondes: 16 16 11 14 13 5 5 4 11 22 15 19

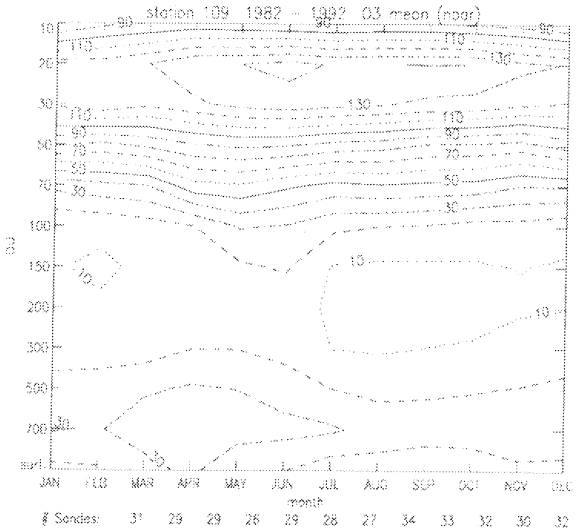
station 109 1982 - 1992 O3 mean (nbar)
DU
month
JAN FEB MAR APR MAY JUN JUL AUG SEP OCT NOV DEC
Sondes: 31 29 29 26 29 28 27 34 33 32 30 32

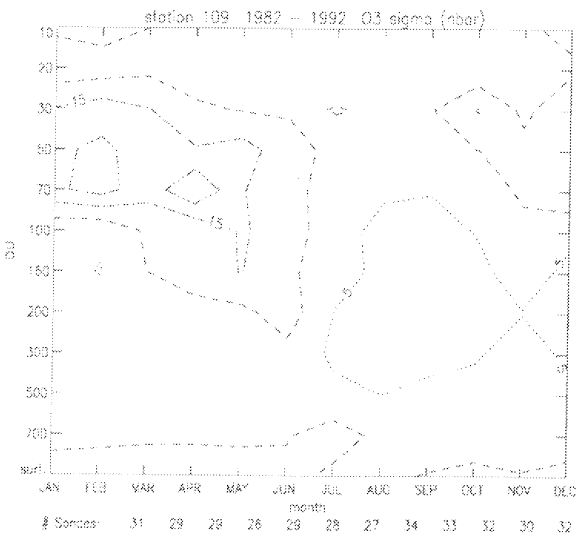
station 109 1982 - 1992 O3 sigma (nbar)
DU
month
JAN FEB MAR APR MAY JUN JUL AUG SEP OCT NOV DEC
Sondes: 31 29 29 26 29 28 27 34 33 32 30 32

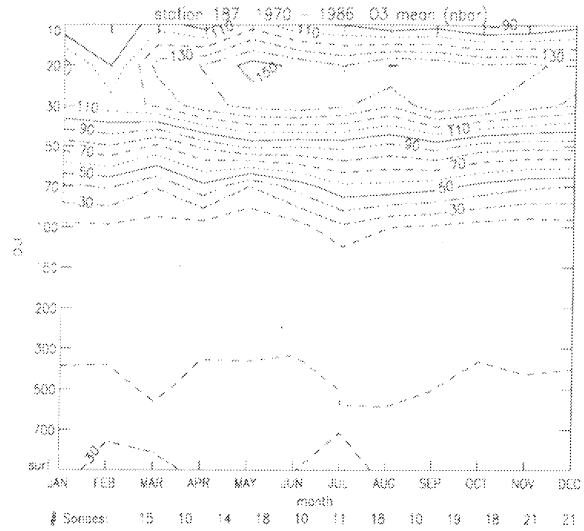
station 187 1970 - 1986 O3 mean (nbar)
hPa
surf
JAN FEB MAR APR MAY JUN JUL AUG SEP OCT NOV DEC
month
Sondes: 15 10 14 18 10 11 18 10 19 18 21 21

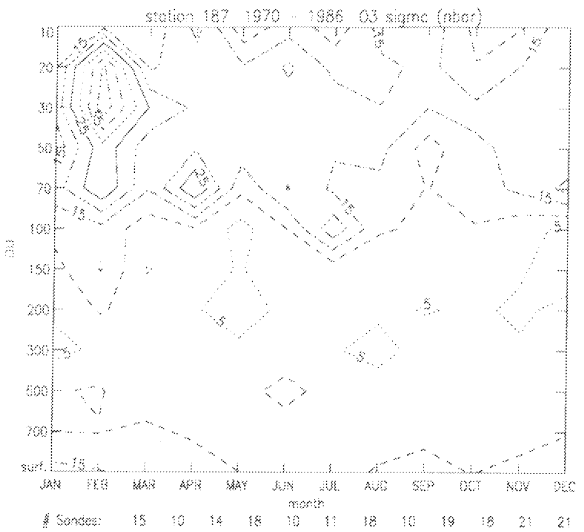
station 187 1970 - 1986 O3 sigma (nbar)
hPa
surf
JAN FEB MAR APR MAY JUN JUL AUG SEP OCT NOV DEC
month
Sondes: 15 10 14 18 10 11 18 10 19 18 21 21

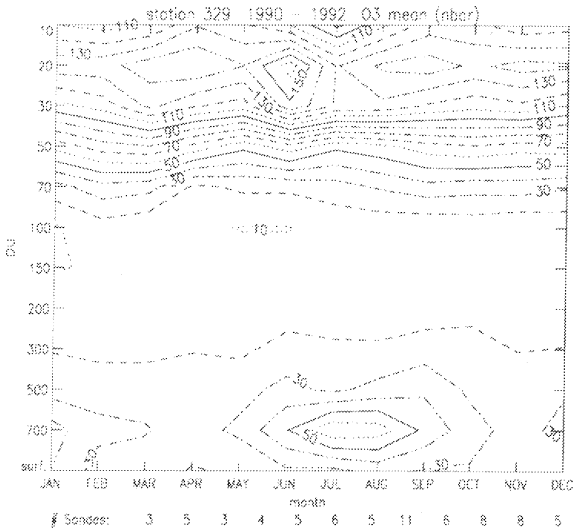
station 329 1990 - 1992 O3 mean (nbar)
hPa
surf
JAN FEB MAR APR MAY JUN JUL AUG SEP OCT NOV DEC
month
Sondes: 3 5 3 4 5 6 5 11 6 8 8 5

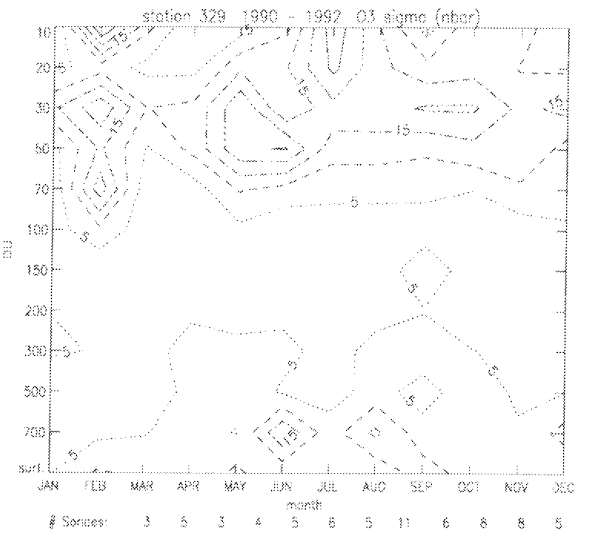
station 329 1990 - 1992 O3 sigma (nbar)
hPa
surf
JAN FEB MAR APR MAY JUN JUL AUG SEP OCT NOV DEC
month
Sondes: 3 5 3 4 5 6 5 11 6 8 8 5

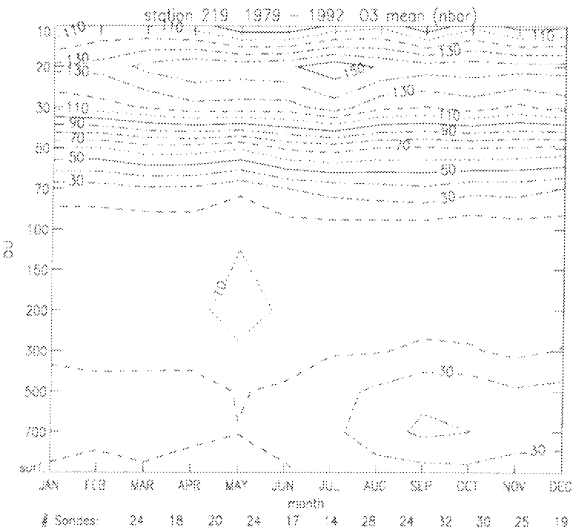
station 219 1979 - 1992 O3 mean (nbar)
hPa
surf
JAN FEB MAR APR MAY JUN JUL AUG SEP OCT NOV DEC
month
Sondes: 24 18 20 24 17 14 28 24 32 30 25 19

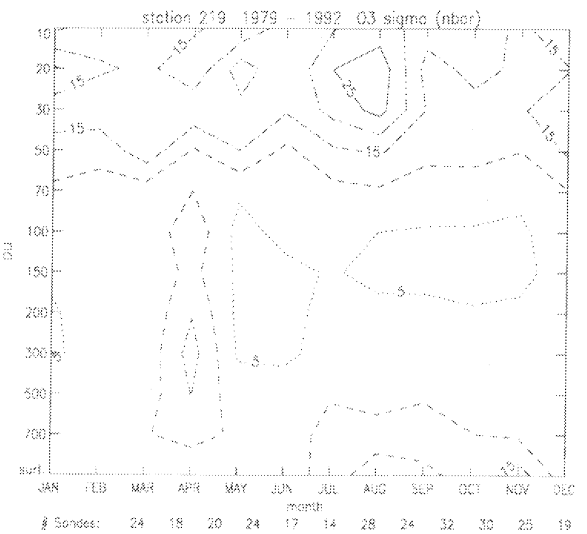
station 219 1979 - 1992 O3 sigma (nbar)
hPa
surf
JAN FEB MAR APR MAY JUN JUL AUG SEP OCT NOV DEC
month
Sondes: 24 18 20 24 17 14 28 24 32 30 25 19

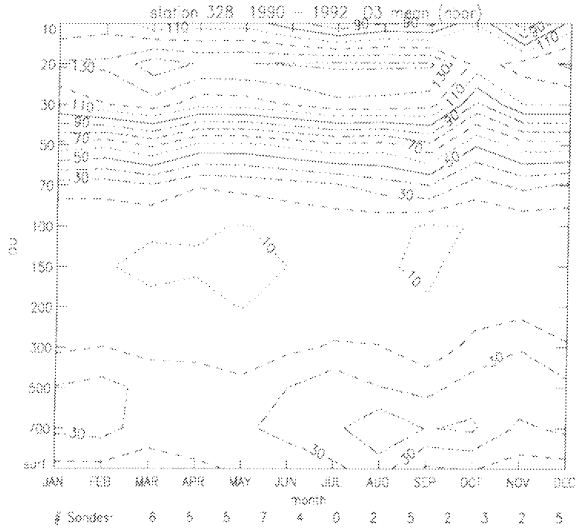
station 328 1990 - 1992 O3 mean (nbar)
DU
month
JAN FEB MAR APR MAY JUN JUL AUG SEP OCT NOV DEC
Sondes: 6 5 5 7 4 0 2 5 2 3 2 5

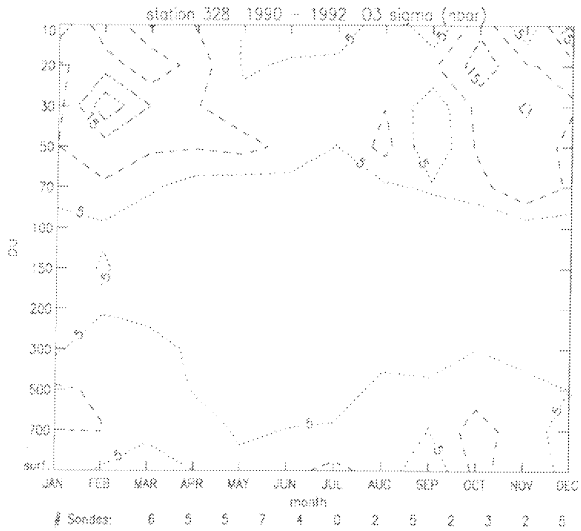
station 328 1990 - 1992 O3 sigma (nbar)
DU
month
JAN FEB MAR APR MAY JUN JUL AUG SEP OCT NOV DEC
Sondes: 6 5 5 7 4 0 2 5 2 3 2 5

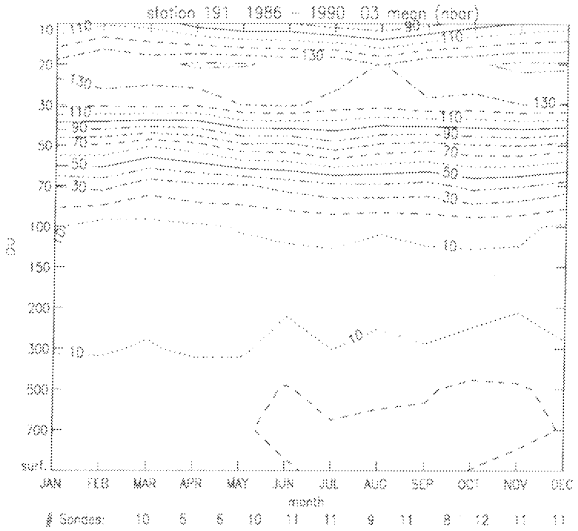
station 191 1986 - 1990 O3 mean (nbar)
DU
month
JAN FEB MAR APR MAY JUN JUL AUG SEP OCT NOV DEC
Sondes: 10 5 5 10 11 11 9 11 8 12 11 11

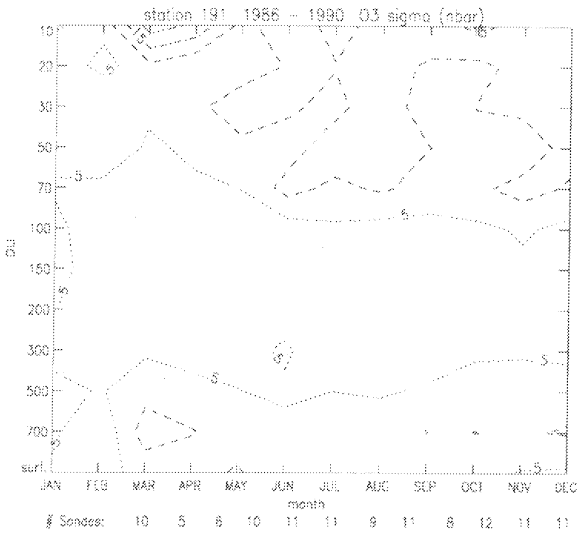
station 191 1986 - 1990 O3 sigma (nbar)
DU
month
JAN FEB MAR APR MAY JUN JUL AUG SEP OCT NOV DEC
Sondes: 10 5 5 10 11 11 9 11 8 12 11 11

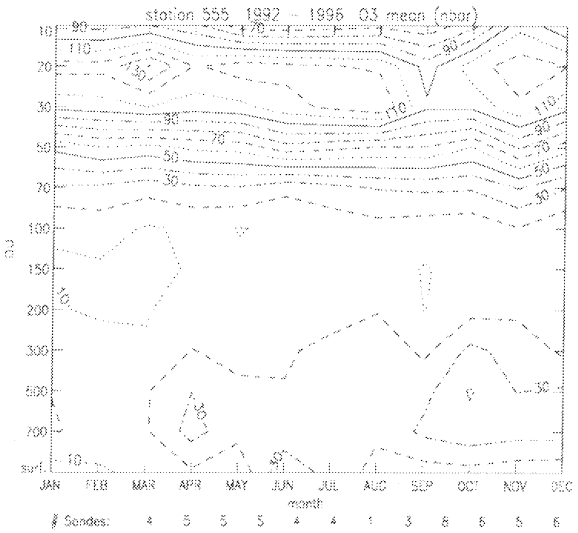
station 555 1992 - 1996 O3 mean (nbar)
DU
month
JAN FEB MAR APR MAY JUN JUL AUG SEP OCT NOV DEC
Sondes: 4 5 5 5 4 4 1 3 8 6 5 6

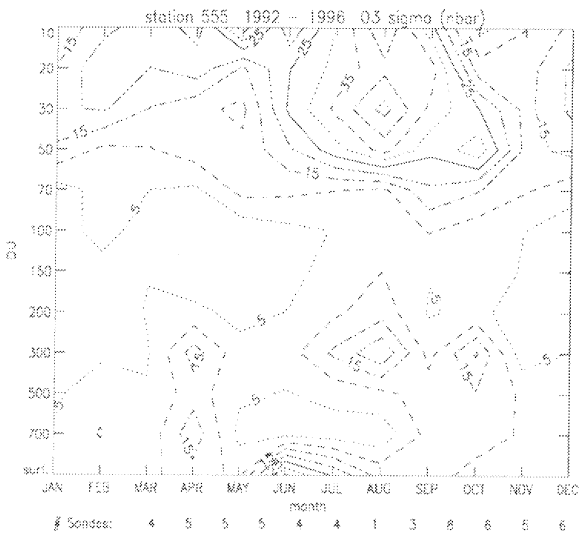
station 555 1992 - 1996 O3 sigma (nbar)
DU
month
JAN FEB MAR APR MAY JUN JUL AUG SEP OCT NOV DEC
Sondes: 4 5 5 5 4 4 1 3 8 6 5 6

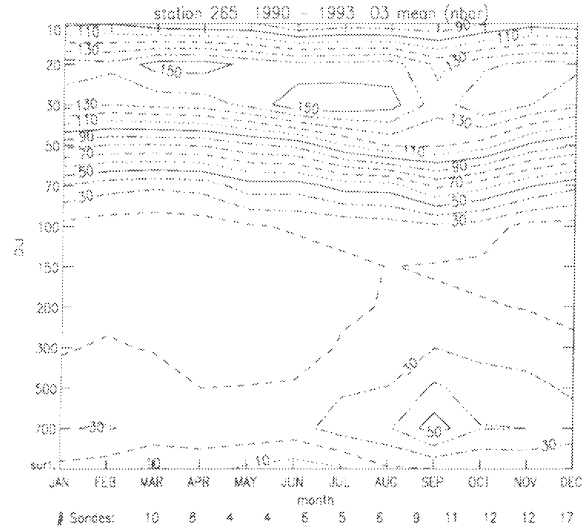
station 265 1990 - 1993 O3 mean (nbar)
DU
JAN FEB MAR APR MAY JUN JUL AUG SEP OCT NOV DEC
month
Sondes: 10 8 4 4 5 5 6 9 11 12 12 17

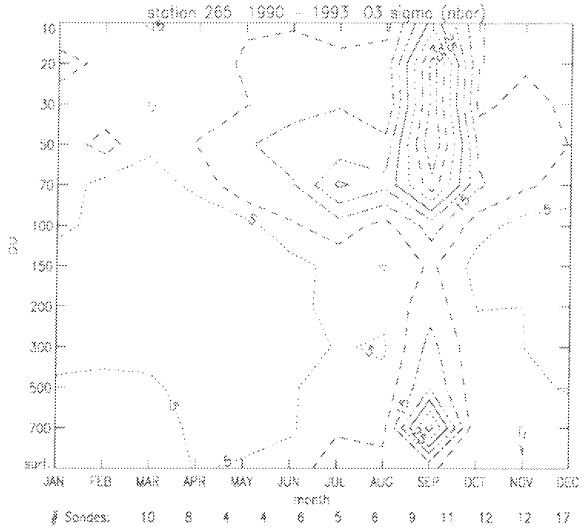
station 265 1990 - 1993 O3 sigma (nbar)
DU
JAN FEB MAR APR MAY JUN JUL AUG SEP OCT NOV DEC
month
Sondes: 10 8 4 4 6 5 6 9 11 12 12 17

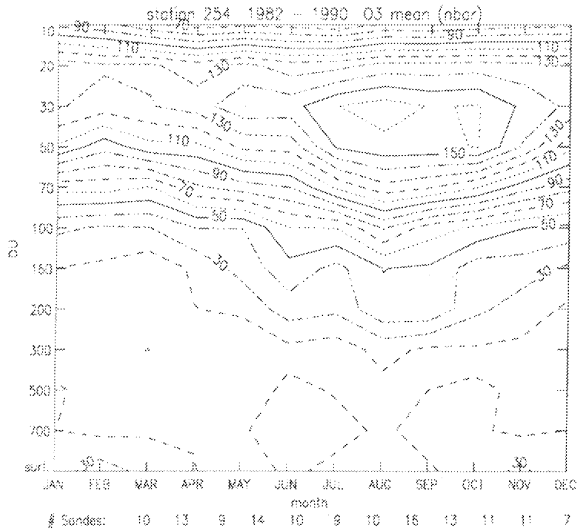
station 254 1982 - 1990 O3 mean (nbar)
DU
JAN FEB MAR APR MAY JUN JUL AUG SEP OCT NOV DEC
month
Sondes: 10 13 9 14 10 9 10 16 13 11 11 7

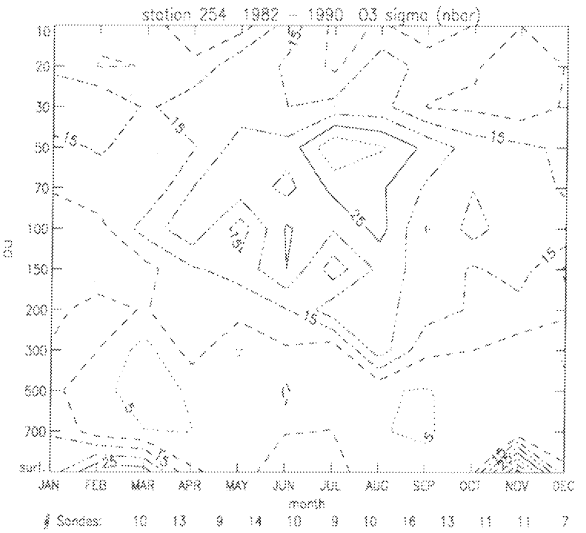
station 254 1982 - 1990 O3 sigma (nbar)
DU
JAN FEB MAR APR MAY JUN JUL AUG SEP OCT NOV DEC
month
Sondes: 10 13 9 14 10 9 10 16 13 11 11 7

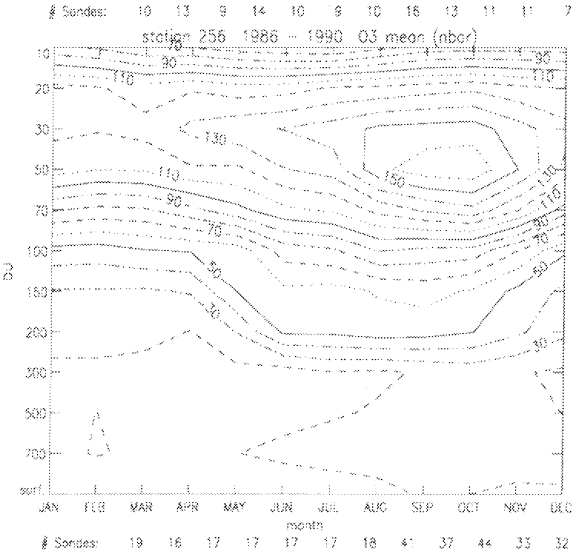
station 256 1986 - 1990 O3 mean (nbar)
DU
JAN FEB MAR APR MAY JUN JUL AUG SEP OCT NOV DEC
month
Sondes: 19 16 17 17 17 17 18 41 37 44 33 32

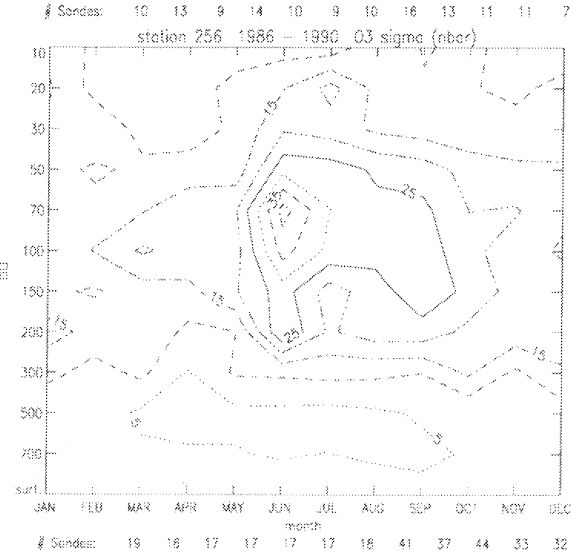
station 256 1986 - 1990 O3 sigma (nbar)
DU
JAN FEB MAR APR MAY JUN JUL AUG SEP OCT NOV DEC
month
Sondes: 19 16 17 17 17 17 18 41 37 44 33 32

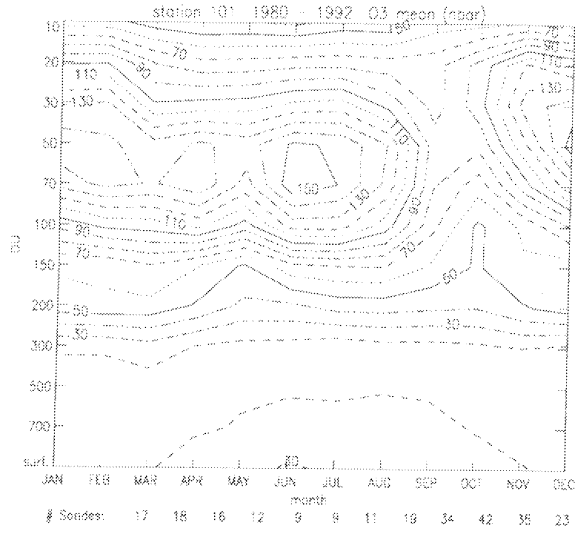
station 101 1980 - 1992 O3 mean (mbar)
mb
month
JAN FEB MAR APR MAY JUN JUL AUG SEP OCT NOV DEC
Sondes: 17 18 16 12 9 9 11 19 34 42 35 23

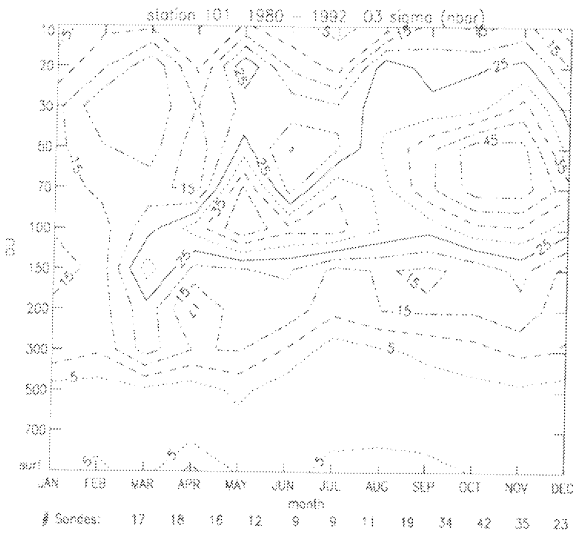
station 101 1980 - 1992 O3 sigma (mbar)
mb
month
JAN FEB MAR APR MAY JUN JUL AUG SEP OCT NOV DEC
Sondes: 17 18 16 12 9 9 11 19 34 42 35 23

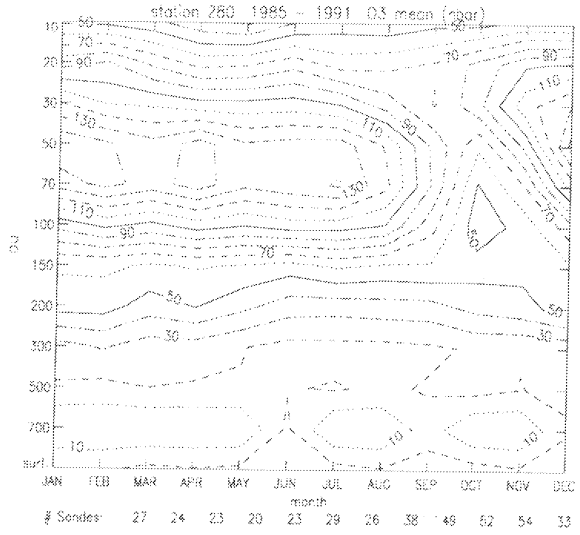
station 280 1985 - 1991 O3 mean (mbar)
mb
month
JAN FEB MAR APR MAY JUN JUL AUG SEP OCT NOV DEC
Sondes: 27 24 23 20 23 29 26 38 49 52 54 33

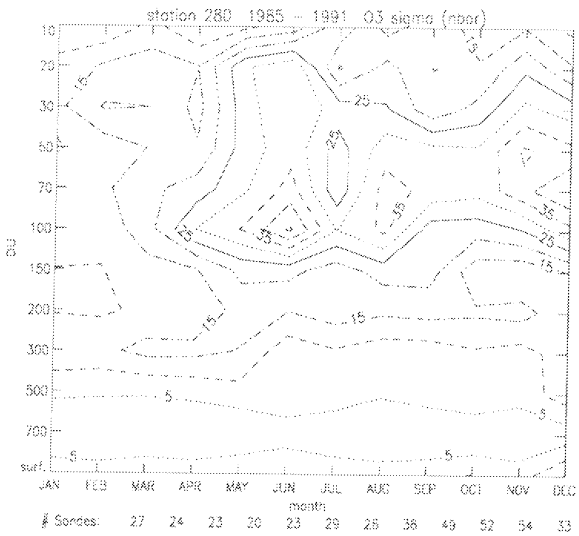
station 280 1985 - 1991 O3 sigma (mbar)
mb
month
JAN FEB MAR APR MAY JUN JUL AUG SEP OCT NOV DEC
Sondes: 27 24 23 20 23 29 26 38 49 52 54 33

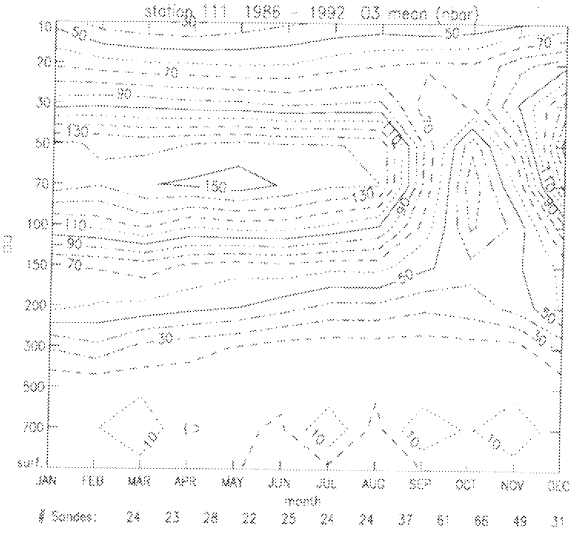
station 111 1986 - 1992 O3 mean (mbar)
mb
month
JAN FEB MAR APR MAY JUN JUL AUG SEP OCT NOV DEC
Sondes: 24 23 28 22 25 24 24 37 61 66 49 31

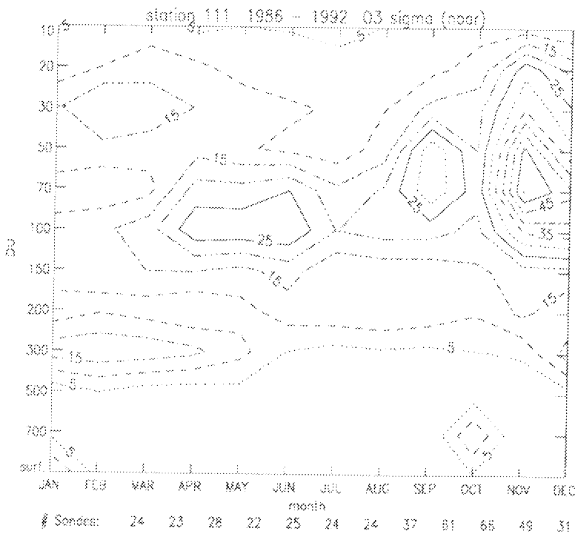
station 111 1986 - 1992 O3 sigma (mbar)
mb
month
JAN FEB MAR APR MAY JUN JUL AUG SEP OCT NOV DEC
Sondes: 24 23 28 22 25 24 24 37 61 66 49 31

Chapter 3

Compilation of Climatology

In compiling the zonal monthly mean climatology, a couple of steps were taken to homogenize the datasets from the ozonesonde stations and incorporate them into the climatology in such a way that the zonal mean state is reflected. This involved scaling the profiles to be consistent with independent datasets of total ozone for the troposphere and for the whole atmosphere, as well as using a weighting technique dependent on latitude and the number of sonde releases per month - as will be discussed in the next sections.

3.1 Total ozone in the troposphere

A digitized dataset of tropospheric total ozone was used to make the tropospheric ozone profiles of the stations between 50° N and 50°S more representative of the zonal mean state. The dataset was obtained by subtracting two satellite datasets from each other, stratospheric ozone recorded by SAGE from total ozone by TOMS over the period 1979-1991, to obtain residual tropospheric ozone (cf. Fishman et al., 1992). The dataset consists of 4 seasonal average ozone distributions on a 5° latitude by 10° longitude grid, and is shown in Fig. 3.1. Clearly, the longitudinal gradients in tropospheric ozone can be quite large, especially near the equator, so that the individual profile of a station need not be representative of the zonal mean profile. To account for this, the tropospheric profile of a station for a given month was multiplied by the ratio of the corresponding zonal average of the Fishman dataset (same latitude and month) over the corresponding grid-box value in which the station is located. To obtain monthly mean values from the seasonal averages of the Fishman dataset, a linear interpolation was performed between the central months of each season - assigning the seasonal average values to the central month. The tropopause height beneath which the scaling was performed was calculated from a simple latitudinal dependence:

$$P_{trop}(t) = 100 + 3 \mid lat \mid + lat.\cos(\frac{2\pi(t-1)}{12}), \quad -50 \leq lat \leq 50 \qquad (3.1)$$

P_{trop} is the tropopause height in hPa, as a function of the month of the year (t=1 to 12); lat is in degrees (North positive). On average, this formula agrees quite well

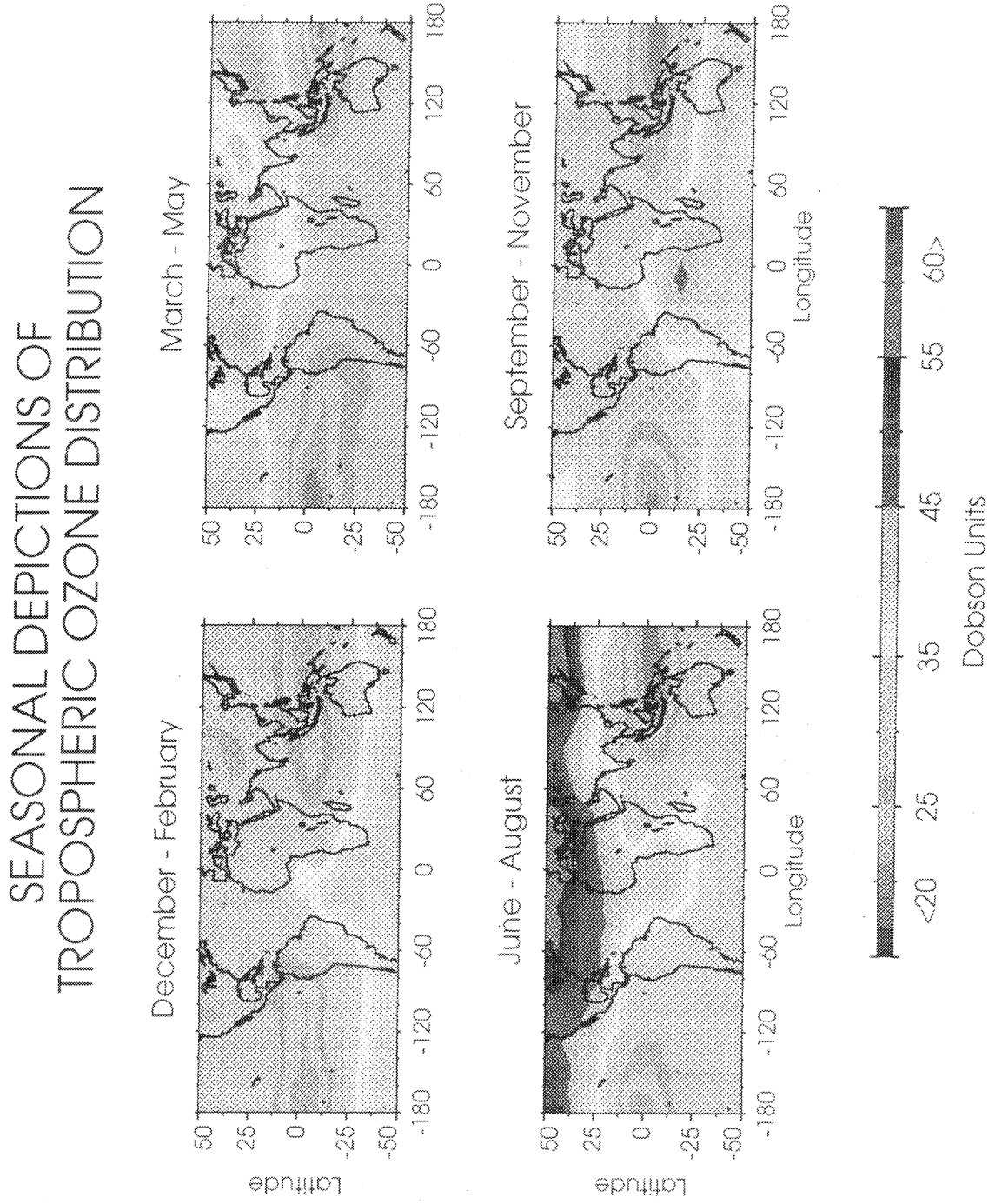

Figure 3.1 Tropospheric residual ozone, taken from Fishman et al. (1990).

with the tropopause height derived from integrating the tropospheric ozone profile for each station until the corresponding total ozone value from the Fishman dataset was reached. Of course, even a scaled tropospheric ozone profile need not be equal to the zonal mean profile, even though its integral is, but as long as satellites can not resolve tropospheric ozone profiles, there is no way to account for this. Besides accounting for longitudinal gradients in the tropospheric ozone of a zonal band, this scaling is also a way to make the station datasets more homogeneous in time, as the period of the Fishman dataset (79-91) almost coincides with the target period set for the climatology (80-91). For the higher latitudes beyond the Fishman dataset region, the tropospheric ozone profiles were left unmodified. This was partly due to the fact that no independent total tropospheric ozone values were available for this region, but also the assumption that the individual profiles are representative of the zonal mean ones becomes more reasonable here - as the zonal bands are shorter and the anthropogenic influence on tropospheric ozone smaller.

3.2 Weighted averaging

Once the tropospheric ozone profiles for each station have been scaled as described above, the zonal means were determined for each of the 17 zonal belts by averaging the stations located within or near a zonal belt in a weighted way. The monthly average profile of each station was weighted with the number of sonde releases performed over the observation period for this month, and with a simple function of the latitudinal distance to the central latitude of the zonal belt:

$$w_{lat} = \frac{25 - \mid lat_{station} - lat_{zone} \mid}{25} \tag{3.2}$$

Before adding the profiles together at the standard pressure levels, the ozone value for the 1000 hPa standard level had to be calculated for the higher elevated stations with lower annual surface pressure values (for the South Pole the ozone value at 700 hPa level also had to be calculated). This was done by assuming the same ozone volume mixing ratio at the 1000 hPa (and 700 hPa) level as at the surface. The stations that were averaged together in this weighted way for each zonal belt in the climatology are listed in Table 3.1. As can be seen, the zone 3 and 10 have no stations within them, so the latitudinal interpolation given above is used for the stations located in the upper and lower neighbouring zonal belts. For zone 13 at Northern midlatitudes, it occurs that stations lie within the same, or in neighbouring gridpoint of the Fishman dataset. To account for this close co-location, an additional weighting of respectively 0.5 and 0.8 was given to these stations, as opposed to a 1.0 weighting for the stations at a more distant reach from each other. The above-mentioned procedure was followed for determining both the zonal mean and the zonal standard deviation fields.

Table 3.1 An overview of the stations used to calculate the zonal mean profile of each zonal band in the ozone climatology

zonal band no.	boundary	station numbers
	85° N	
17		18, 89
	75° N	
16		24, 262
	65° N	
15		262, 77, 21
	55° N	
14		21, 76, 221, 174, 99, 156
	45° N	
13		197, 12, 67, 107, 14
	35° N	
12		14, 7, 109
	25° N	
11		109, 187
	15° N	
10		329, 187, 109
	5° N	
9		219, 329
	5° S	
8		219, 328, 191
	15° S	
7		265, 555, 191
	25° S	
6		555, 265, 254
	35° S	
5		254, 256
	45° S	
4		256
	55° S	
3		256, 101
	65° S	
2		280, 101
	75° S	
1		280, 111
	85° S	

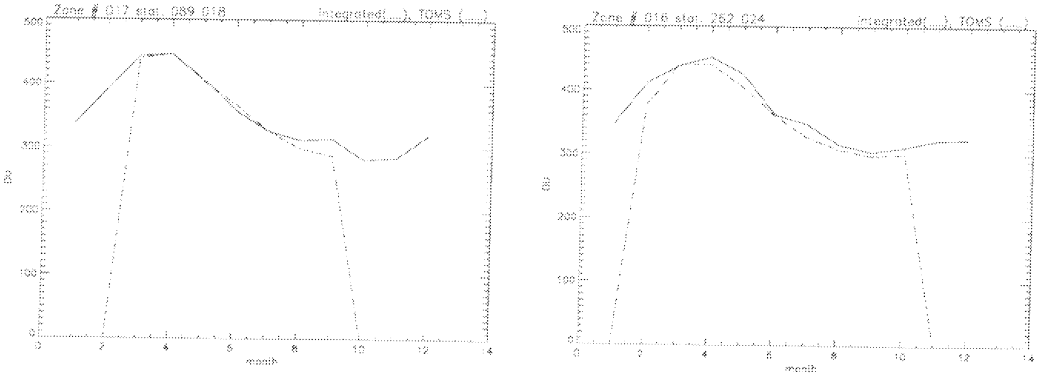

Figure 3.2 Above and following 2 pages: Comparison of the integrated zonal mean ozone profiles (solid lines), for zonal bands 1-17, with TOMS version 7 data (dash-dot line) over 1980-1991. The zonal band number and the stations which comprise the band (cf. Table 3.1), are indicated above each plate

3.3 Total ozone in the atmosphere

In a final consistency check, the integrated mean profiles of the 17 zonal belts were compared with TOMS (version 7) zonal monthly means over the period 1980-1991. The formula used to integrate the zonal mean profiles is based on the hydrostatic equation, and basically adds together the products of the ozone volume mixing ratio (MR_k, in ppmv) and the layer thickness (ΔP_k, in hPa), for each layer:

$$Tot.O_3 = 0.79 \sum_{k=1}^{top} MR_k \, \Delta P_k \tag{3.3}$$

If the recorded profile did not reach to the top standard pressure layer, a constant mixing ratio equal to the last recorded value was assumed for all the layers above it - a procedure standardly followed when concurrent total ozone measurements are made to determine the correction factor. The above formula was found to agree closely in most cases where such independent total ozone measurements. Fig. 3.2 shows how well the integrated zonal mean profile agree with the corresponding TOMS values for each month of the year. As can be seen, the NH zonal bands at mid to high latitudes show a good agreement with TOMS. However, things clearly go wrong around the equator, for bands 8 and 9, where the integrated values systematically exceeds the TOMS values - by as much as 50 DU. This is kind of surprising, as the quite extensive Natal dataset is incorporated in these two zonal belts. However, no concurrent total ozone measurements were performed over the observation period of Natal or the other equatorial stations, making it hard to pinpoint the reason for such large errors. Towards the higher SH latitudes, the agreement improves again, except for zonal belt 3, where the integrated values underestimate TOMS values. This is probably due to the influence of Syowa station on Antarctica, which was combined with Lauder station to produce this zonal average. For the lowermost two zonal

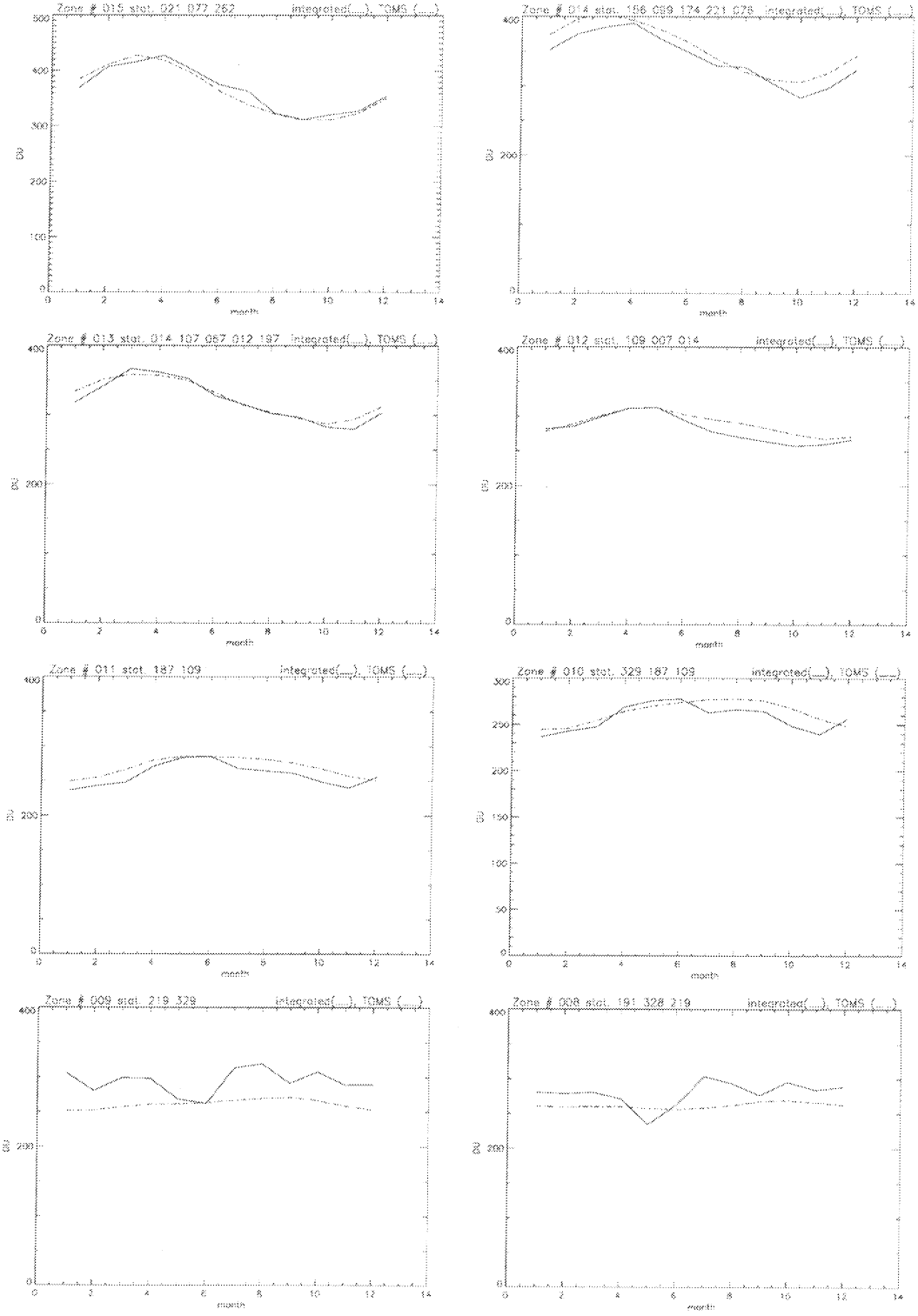
Zone # 015 stat. 021 077 262 integrated( ), TOMS ( )
Zone # 014 stat. 156 089 174 221 078 integrated( ), TOMS ( )
Zone # 013 stat. 014 107 057 012 197 integrated( ), TOMS ( )
Zone # 012 stat. 109 007 014 integrated( ), TOMS ( )
Zone # 011 stat. 187 109 integrated( ), TOMS ( )
Zone # 010 stat. 329 187 109 integrated( ), TOMS ( )
Zone # 009 stat. 219 329 integrated( ), TOMS ( )
Zone # 008 stat. 191 328 219 integrated( ), TOMS ( )
DU
month

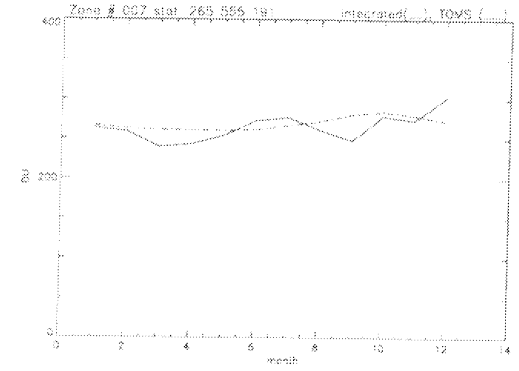
Zone # 007 stat 265 556 (9)
Integrated( ), TOMS ( )
DU
month

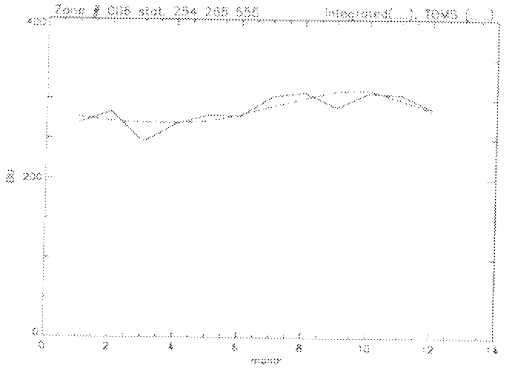
Zone # 008 stat 254 265 556
Integrated( ), TOMS ( )
DU
month

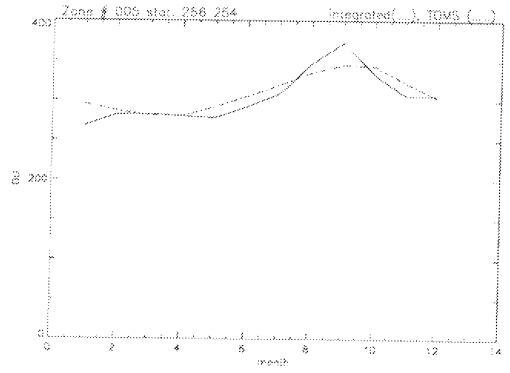
Zone # 005 stat 256 254
Integrated( ), TOMS ( )
DU
month

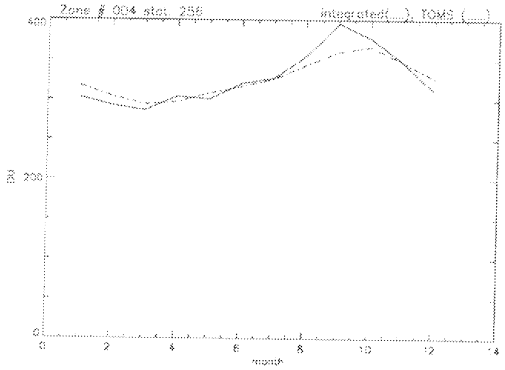
Zone # 004 stat 256
Integrated( ), TOMS ( )
DU
month

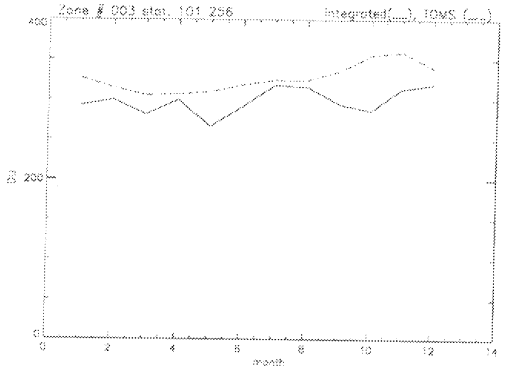
Zone # 003 stat 101 256
Integrated( ), TOMS ( )
DU
month

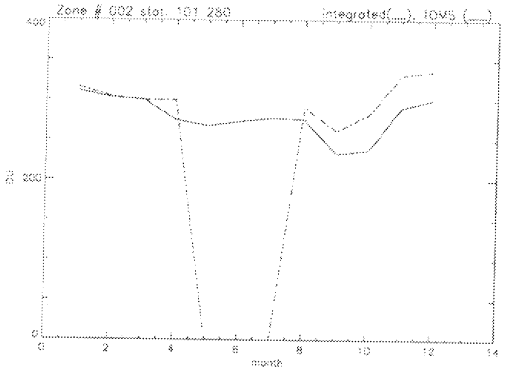
Zone # 002 stat 101 280
Integrated( ), TOMS ( )
DU
month

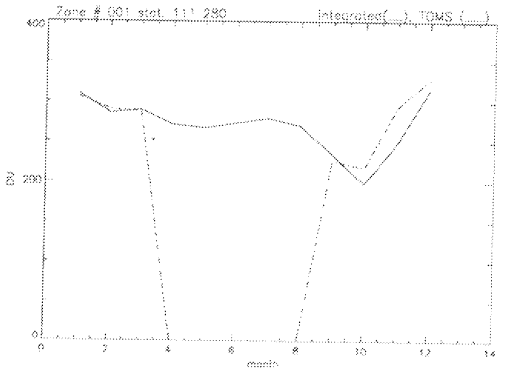
Zone # 001 stat 111 280
Integrated( ), TOMS ( )
DU
month

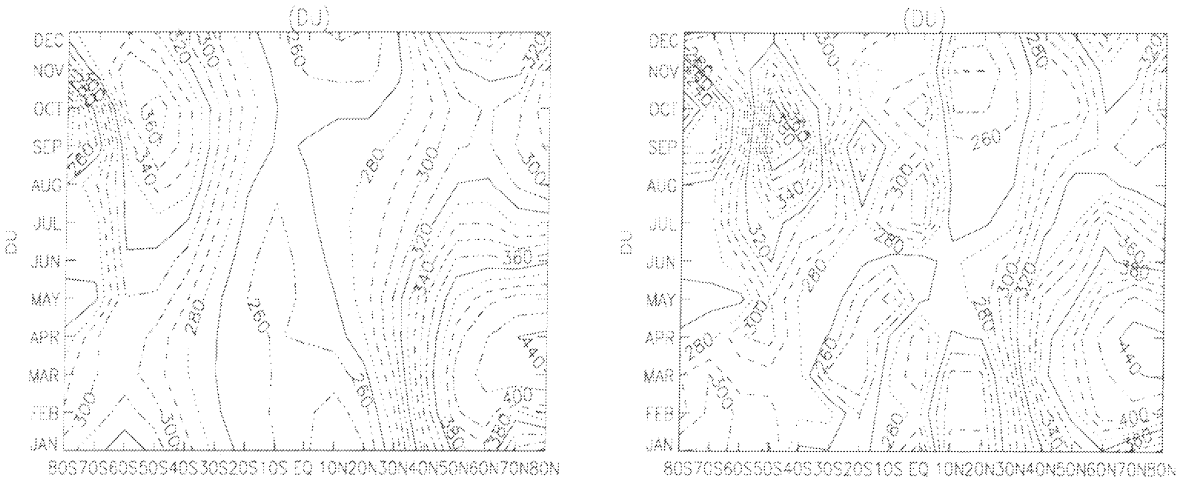

Figure 3.3 Time-latitude distributions of total ozone, obtained by integrating the ozone climatology profiles, before (left panel) and after (right panel) applying a correction with TOMS data over 1980-1991.

bands, the agreement in late summer is quite good, but clearly falls short of the TOMS measurements during the ozone hole period in spring and early summer. This can be due to the later observation periods of the South Pole (86-92) and Forster (85-91), when the ozone hole was at a more developed stage than would be reflected from the average over the target period 80-91.

The last step was to apply the correction factor, obtained from dividing the TOMS values with the integrated zonal mean profiles, to each value of the corresponding profiles and combine the zonal mean and standard deviation fields into one climatology. Fig. 3.3 shows the difference between the TOMS-corrected climatology and the uncorrected version. As TOMS can not measure in the polar nights, no correction was applied to these profiles. The agreement between these two versions are quite good for the higher latitudes, but there is a clear problem on the SH-side of the equator, as pointed out earlier. The result of combining the TOMS-corrected zonal belts into one climatology will be presented and discussed in the next chapter.

Chapter 4

Discussion

After each of the 17 zonal belts were made consistent with the TOMS data, they were appended to each other to form a climatology of the zonal monthly mean ozone. The same correction factors applied to the station and zonal mean ozone profiles were applied to the corresponding standard deviation profiles, and were combined in a similar way to form a standard deviation climatology. As an overview, the annual mean and standard deviation climatology are shown in Fig. 4.1, for partial pressure (nbar) and volume mixing ratio (parts per billion by volume, or ppbv) units. The monthly mean climatologies are given in Fig. 4.2 (nbar), and Fig. 4.3 (ppbv). As mentioned earlier, the partial pressure units provide more insight into the dynamics associated with the ozone distribution, whereas the mixing ratio indicates more where the sources and sinks of ozone are active. One of the clearest ways to illustrate this is to compare the locations of maximum mean ozone concentrations for both units. When viewed in partial pressure (Fig. 4.2), the maximal mean ozone values are located around 70 hPa at NH polar latitudes during the spring season, due to the buildup of ozone transported from the equator by the intensified Hadley circulation in NH winter (this is not true for the SH poles due to the ozone hole phenomenon). When viewed in partial pressure (Fig. 4.3), the maximum is located at the top pressure layer around the equator, where the solar insolation, and hence the production of ozone, is maximal. Also apparent from the mixing ratio plot is the ozone production signal most likely associated with biomass burning at the end of the SH winter, stretching from the equator southward during September and later shifting more towards SH midlatitudes during October and November. The on-average higher tropospheric ozone mixing ratios in the NH than SH is also evidence of high ozone production through smog in the summer months (Fig. 4.3), or due to an increased influx from the stratosphere in the spring months.

When viewing the standard deviation (square root of the variance) plots, different features also become apparent when viewed in either nbar of ppbv. For partial pressure the maximum variance occurs in the NH just below the altitude of maximum mean ozone at polar latitudes, which is the region where the variability in ozone is the largest due to the high dynamical variability of the tropopause region directly below combined with the high ozone concentration from directly above (again, for the SH polar region

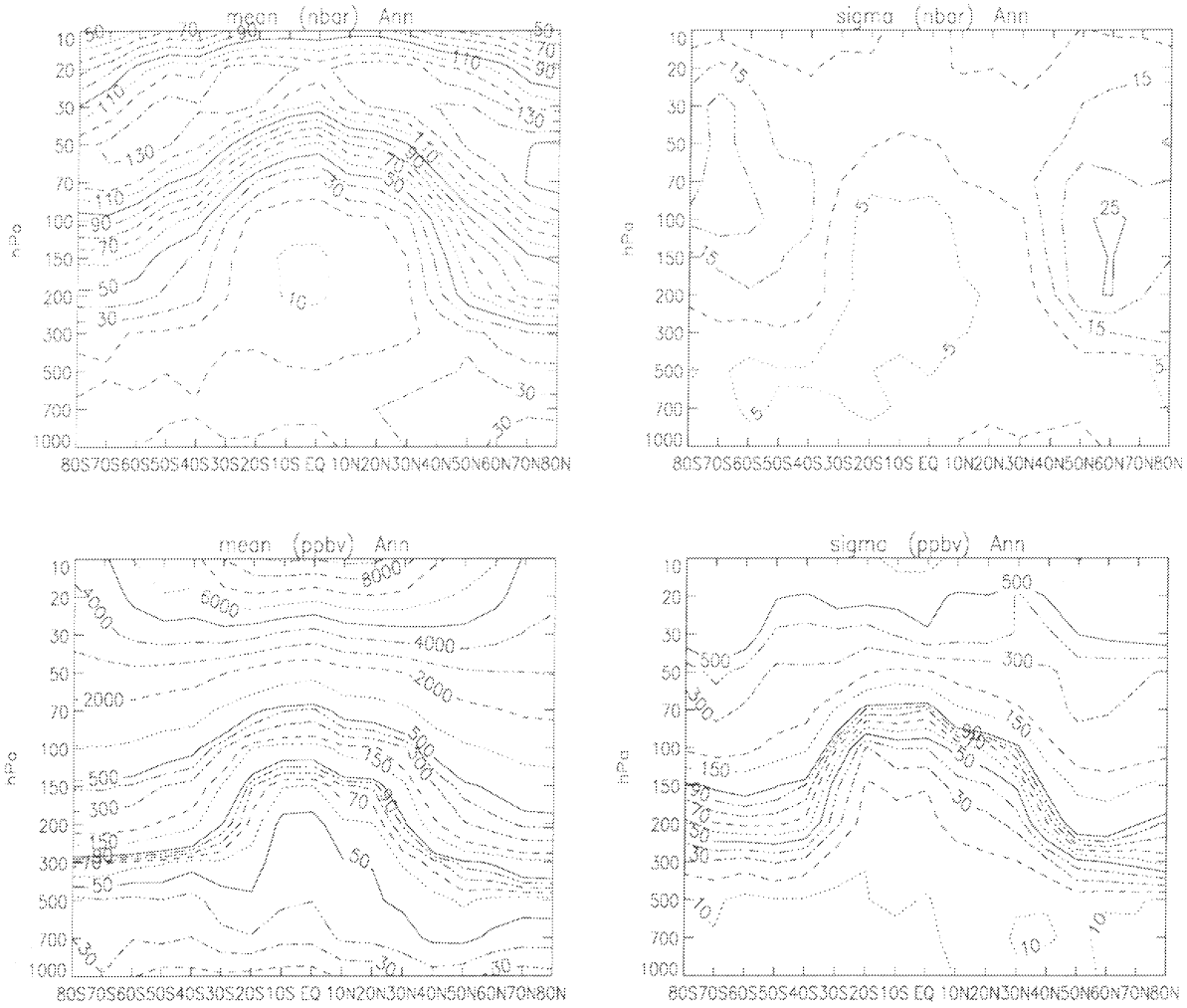

Figure 4.1 Pressure-latitude distributions of the ozone climatology, for annaul mean ozone and its standard deviation, in nbar (top 2 plates) and ppbv (bottom 2 plates).

the situation is different; due to the ozone hole the maximum variance now occur where the maximum mean concentration should have been, at 70 hPa). Viewed in mixing ratios, the maximum variance occur at higher altitudes now associated with variation in ozone production or destruction. Care should however be taken not to equate the variance to the natural variability alone, as the variance is also inversely proportional to the length of the time series it is calculated from. Hence, the the corresponding station observation periods should be kept in mind to discriminate between the natural variability and the reliability of the mean ozone values.

As pointed out in the previous chapter, the equatorial zonal belt (no. 9) showed a large discrepancy between the integrated zonal mean profiles and the corresponding TOMS data. This resulted in a large correction factor for the equatorial belt, such that the scaled down profile values become visible as a kink in the isopleths of

mean ozone at higher altitudes, for all months except May and June. This is unlikely to be a natural feature, and an alternative would be to use the uncorrected profiles. However, then the discrepancy with the TOMS data is a problem. As no concurrent ground-based total ozone observations were performed for any of the equatorial stations, the best solution would be to compare each recorded profile in time with the closest possible TOMS observation and calculate the corresponding correction factor, after which the averaging is performed. Another option would be to append a satellite-based stratospheric dataset to to the existing climatology, as was done in the previous version (Fortuin and Langematz, 1994), to have a more accurate assessment of the total integrated ozone here (in stead of assuming constant mixing ratio above the last recorded value). Also, one can then determine whether the uncorrected or rather the TOMS-corrected version is most likely to be true, based on the agreement within the overlap region (P-layers from 70 to 10 hPa) between the ozonesonde climatology and its satellite counterpart. Such an extension is planned in the near future.

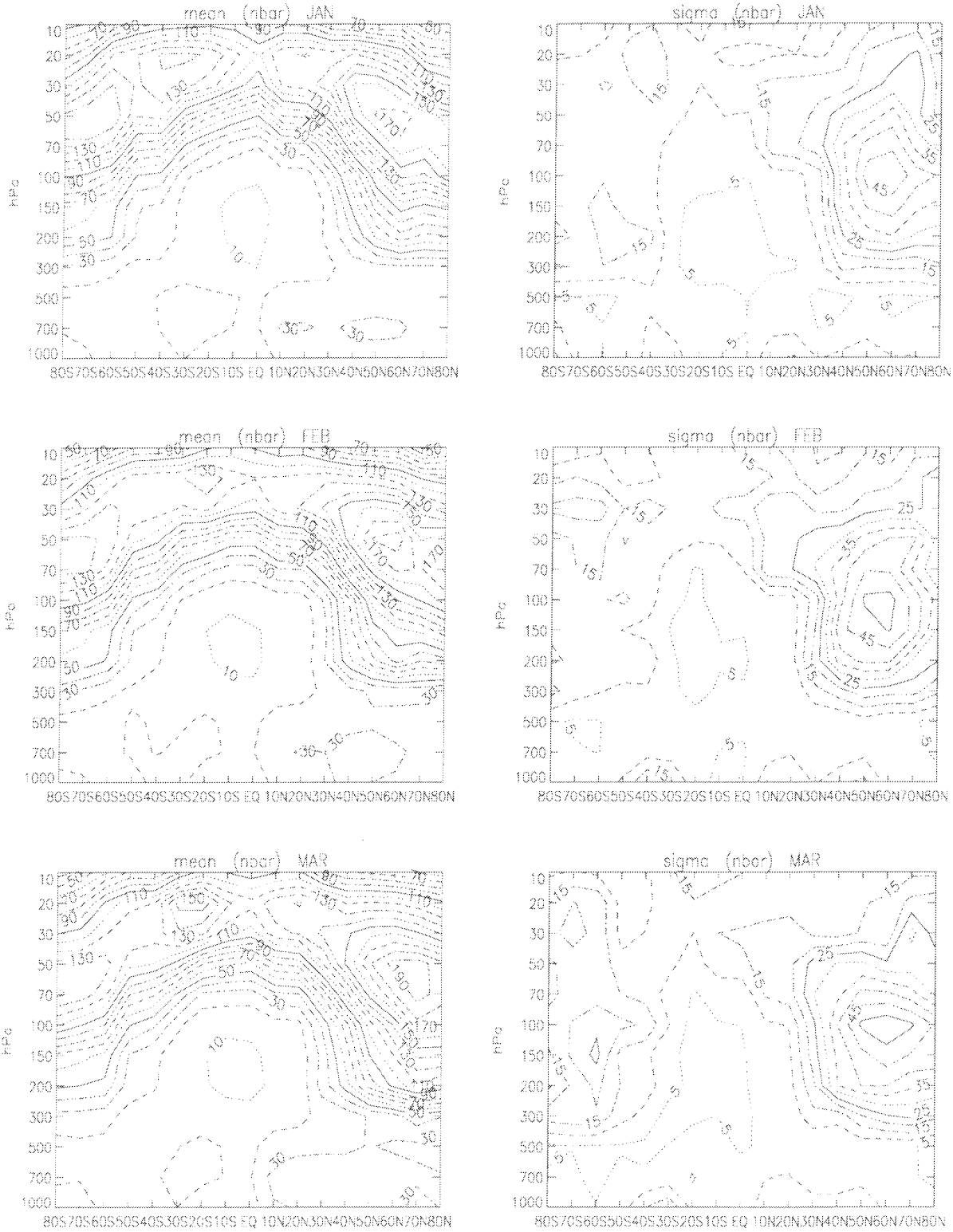

Figure 4.2 Above and following pages: Pressure-latitude distributions (in nbar) of the ozone climatology, for mean ozone concentration and its standard deviation, plotted for each month of the year

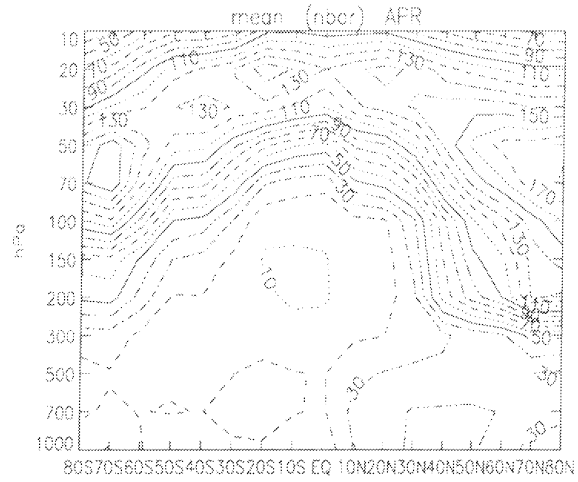
mean (nbar) APR
hPa
80S70S60S50S40S30S20S10S EQ 10N20N30N40N50N60N70N80N

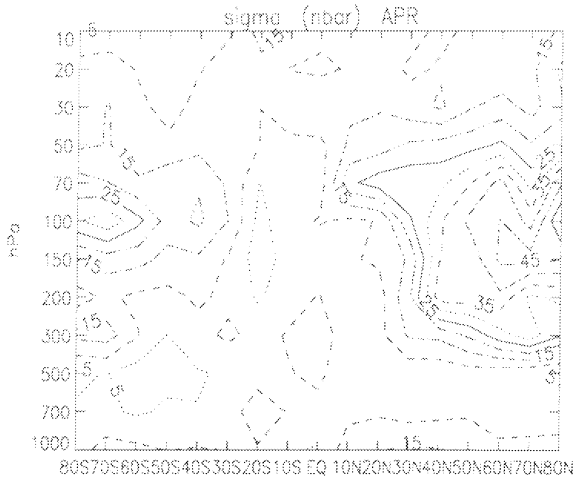
sigma (nbar) APR
hPa
80S70S60S50S40S30S20S10S EQ 10N20N30N40N50N60N70N80N

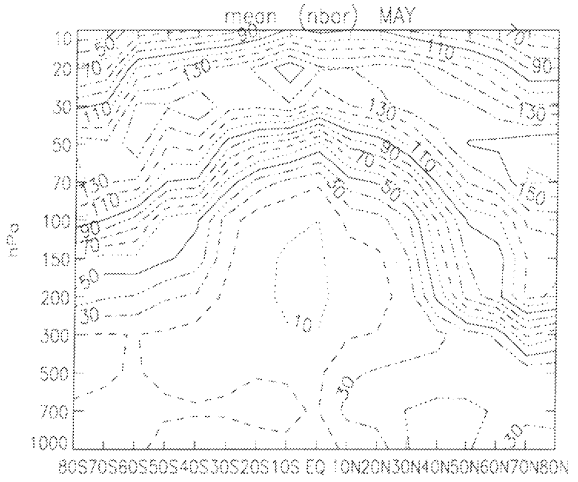
mean (nbar) MAY
hPa
80S70S60S50S40S30S20S10S EQ 10N20N30N40N50N60N70N80N

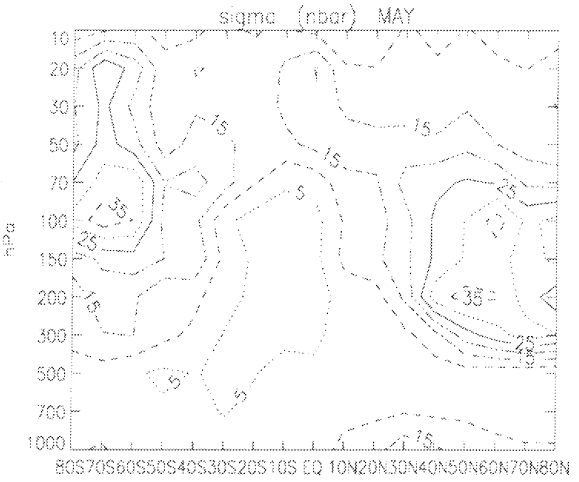
sigma (nbar) MAY
hPa
80S70S60S50S40S30S20S10S EQ 10N20N30N40N50N60N70N80N

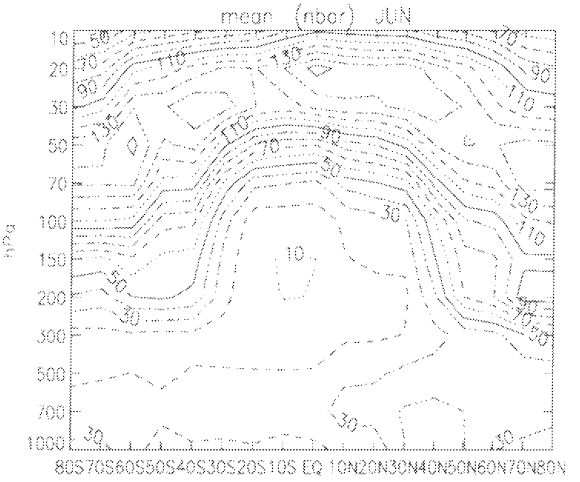
mean (nbar) JUN
hPa
80S70S60S50S40S30S20S10S EQ 10N20N30N40N50N60N70N80N

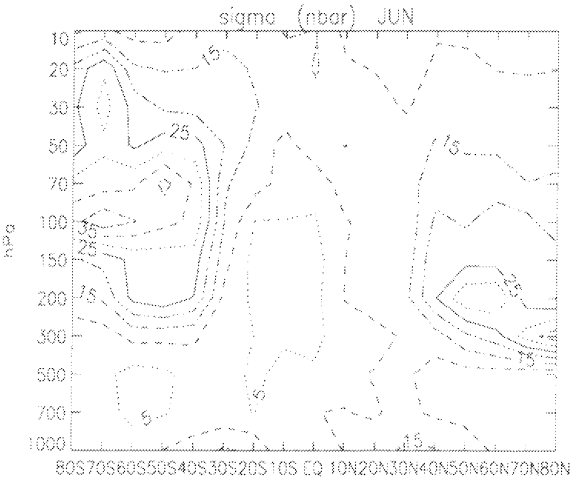
sigma (nbar) JUN
hPa
80S70S60S50S40S30S20S10S EQ 10N20N30N40N50N60N70N80N

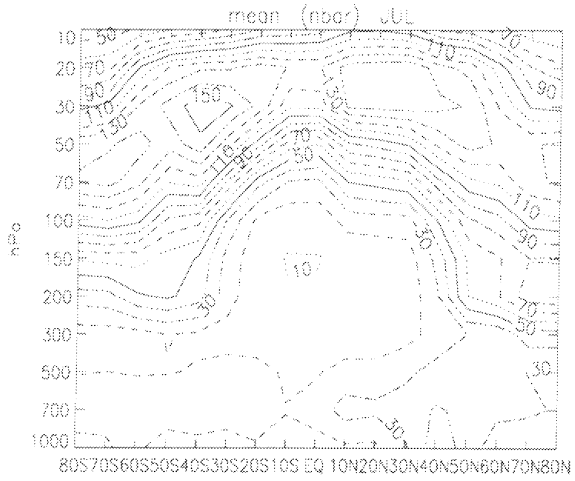
mean (nbar) JUL
hPa
80S70S60S50S40S30S20S10S EQ 10N20N30N40N50N60N70N80N

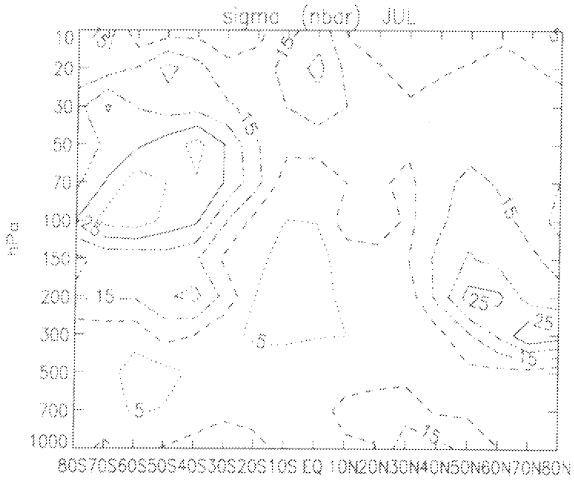
sigma (nbar) JUL
hPa
80S70S60S50S40S30S20S10S EQ 10N20N30N40N50N60N70N80N

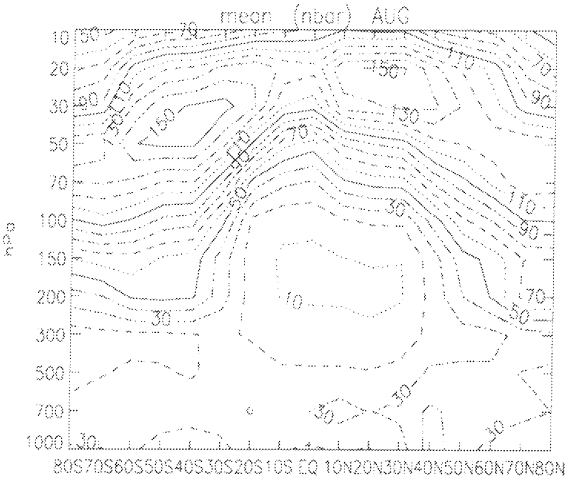
mean (nbar) AUG
hPa
80S70S60S50S40S30S20S10S EQ 10N20N30N40N50N60N70N80N

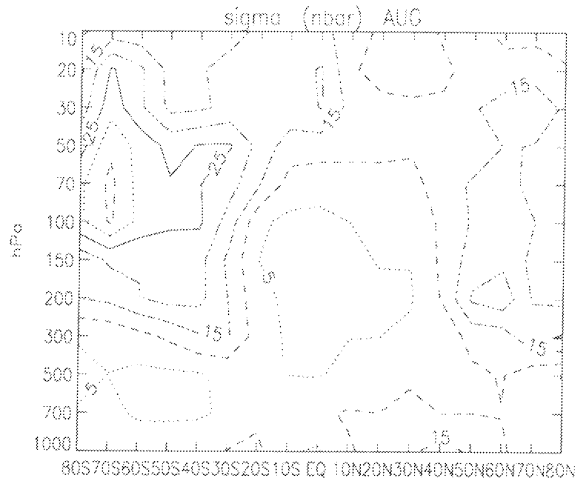
sigma (nbar) AUG
hPa
80S70S60S50S40S30S20S10S EQ 10N20N30N40N50N60N70N80N

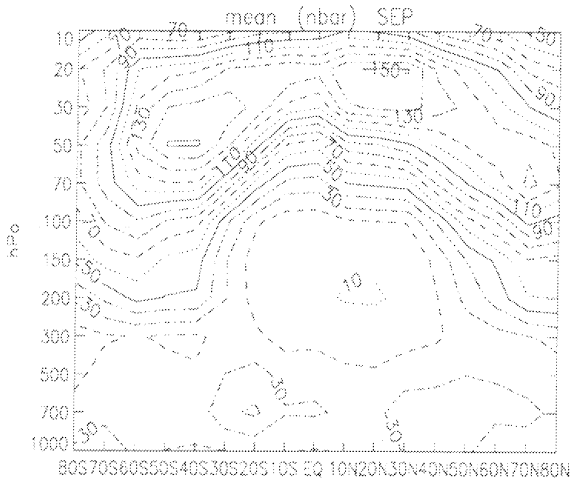
mean (nbar) SEP
hPa
80S70S60S50S40S30S20S10S EQ 10N20N30N40N50N60N70N80N

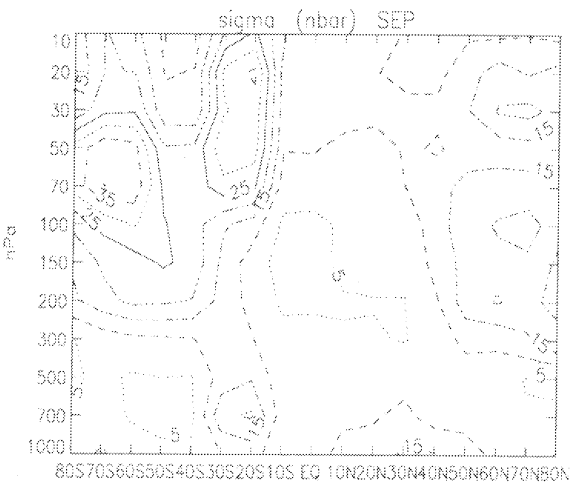
sigma (nbar) SEP
hPa
80S70S60S50S40S30S20S10S EQ 10N20N30N40N50N60N70N80N

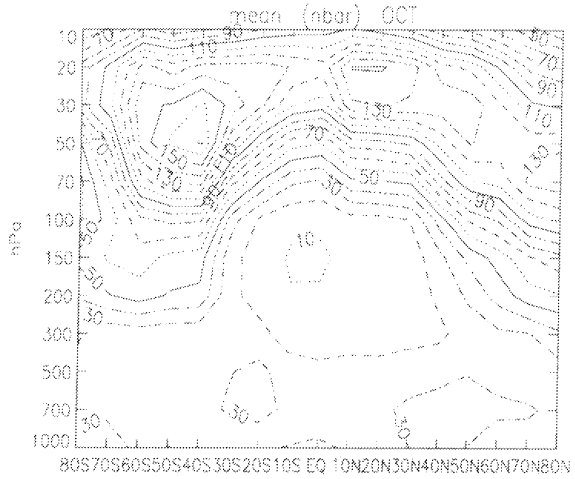
mean (nbar) OCT
hPa
80S70S60S50S40S30S20S10S EQ 10N20N30N40N50N60N70N80N

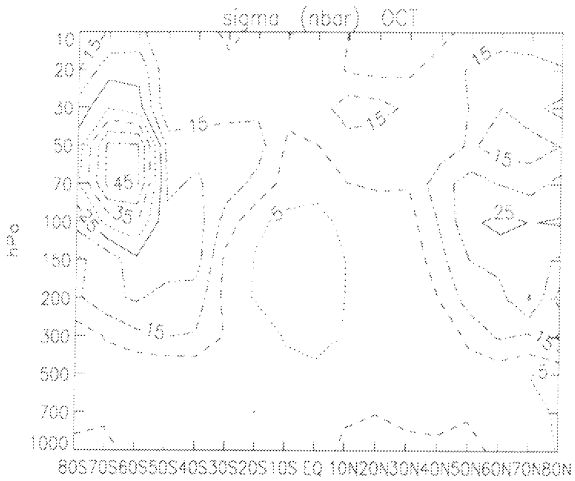
sigma (nbar) OCT
hPa
80S70S60S50S40S30S20S10S EQ 10N20N30N40N50N60N70N80N

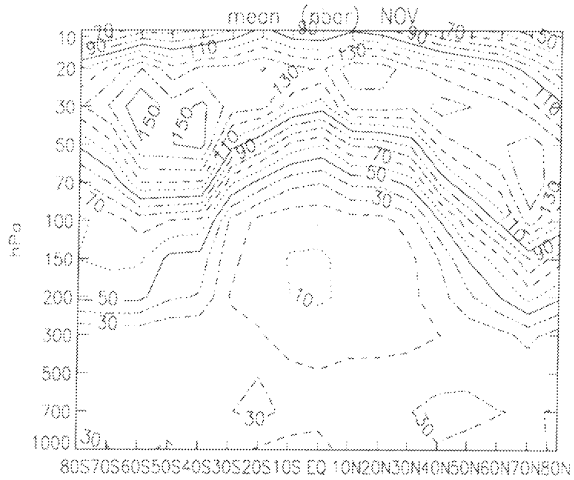
mean (nbar) NOV
hPa
80S70S60S50S40S30S20S10S EQ 10N20N30N40N50N60N70N80N

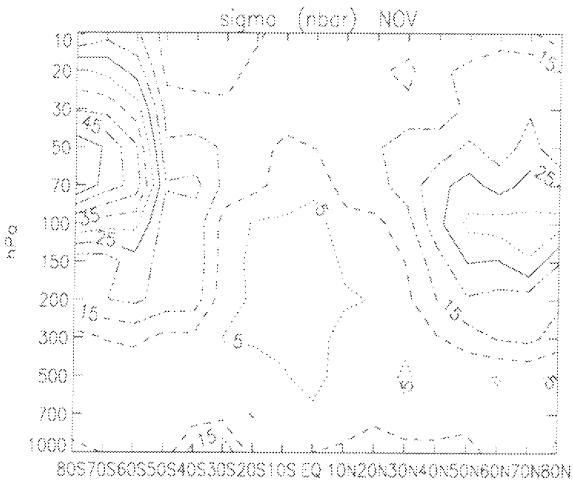
sigma (nbar) NOV
hPa
80S70S60S50S40S30S20S10S EQ 10N20N30N40N50N60N70N80N

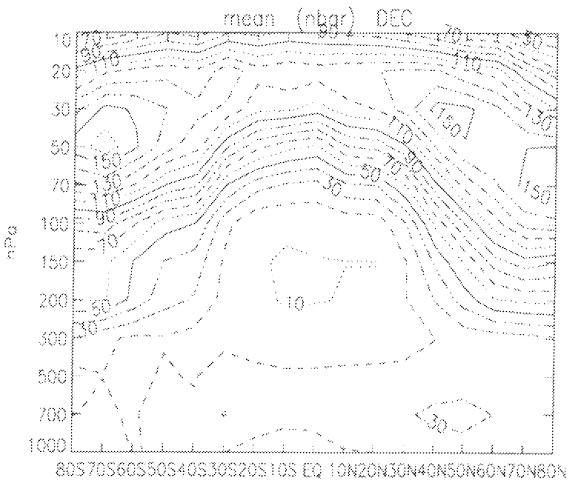
mean (nbar) DEC
hPa
80S70S60S50S40S30S20S10S EQ 10N20N30N40N50N60N70N80N

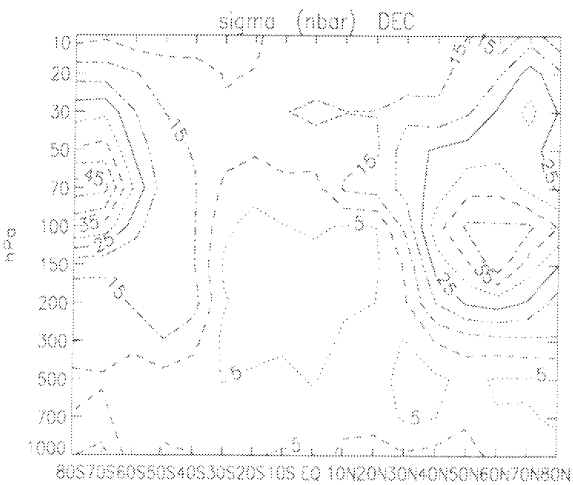
sigma (nbar) DEC
hPa
80S70S60S50S40S30S20S10S EQ 10N20N30N40N50N60N70N80N

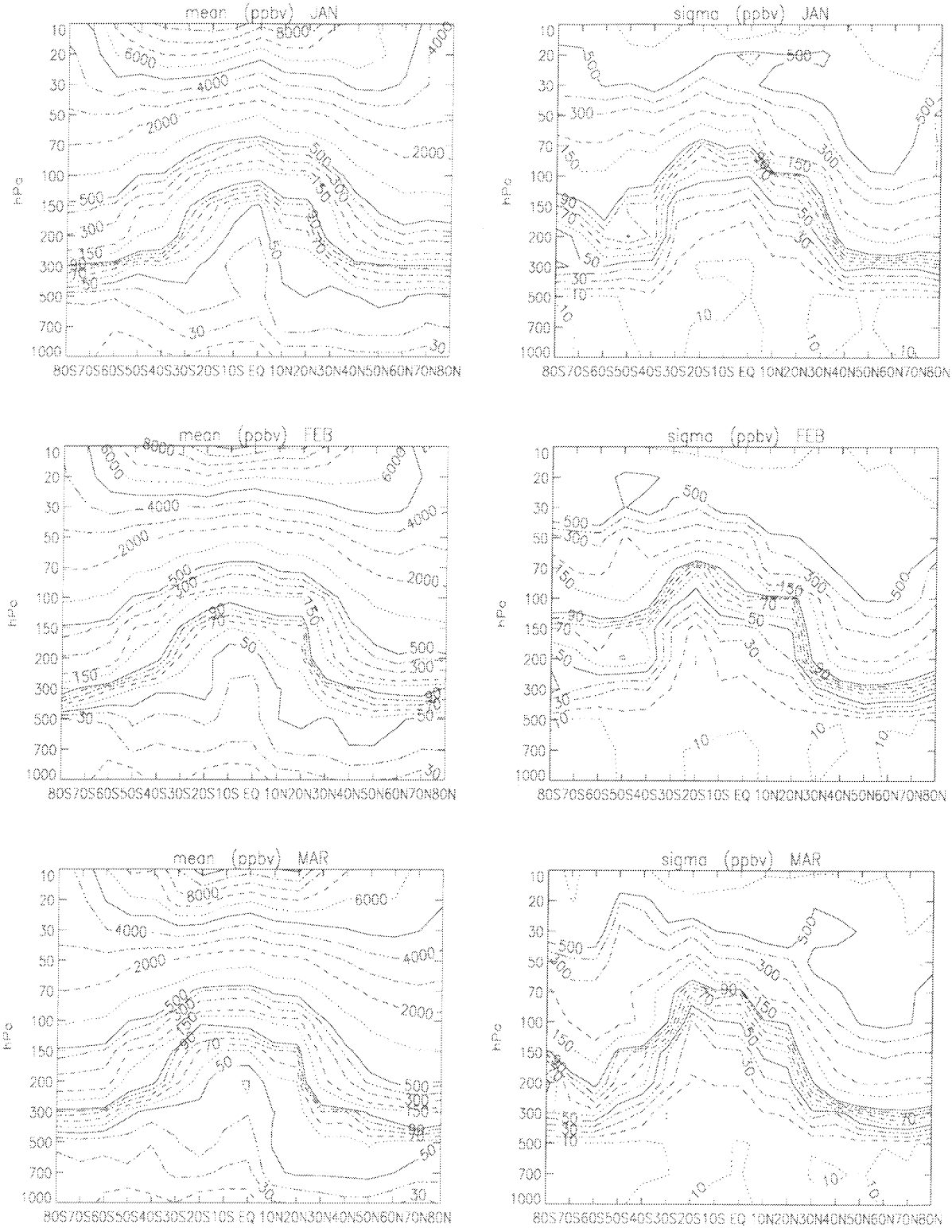

Figure 4.3 Above and following pages: Pressure-latitude distributions (in ppbv) of the ozone climatology, for mean ozone concentration and its standard deviation, plotted for each month of the year

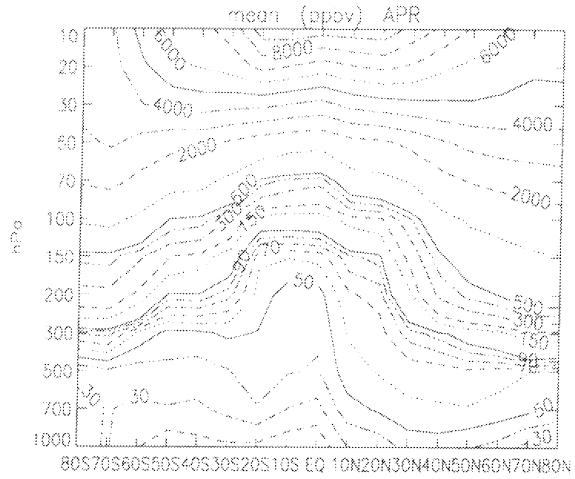
mean (ppbv) APR
hPa
80S70S60S50S40S30S20S10S EQ 10N20N30N40N50N60N70N80N

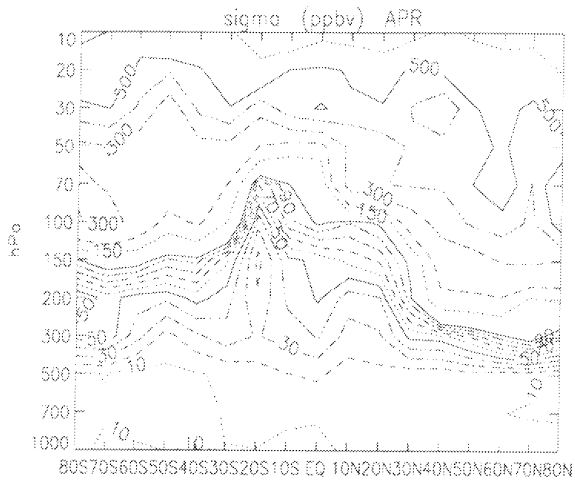
sigma (ppbv) APR
hPa
80S70S60S50S40S30S20S10S EQ 10N20N30N40N50N60N70N80N

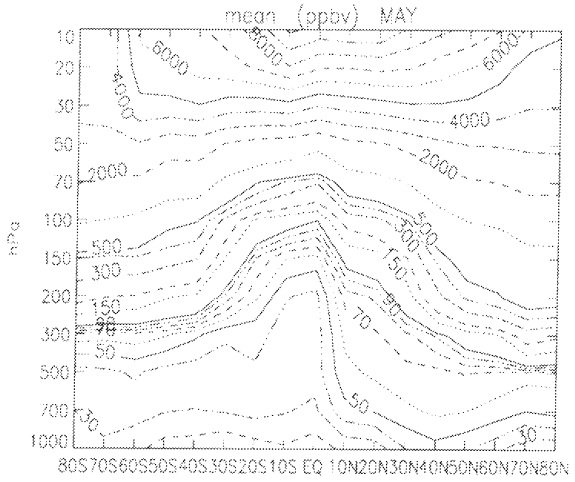
mean (ppbv) MAY
hPa
80S70S60S50S40S30S20S10S EQ 10N20N30N40N50N60N70N80N

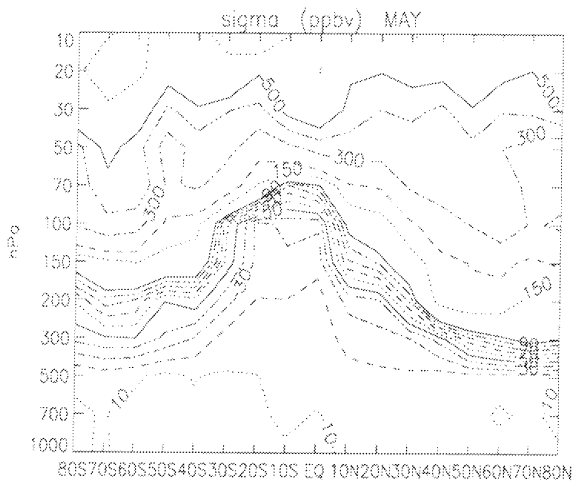
sigma (ppbv) MAY
hPa
80S70S60S50S40S30S20S10S EQ 10N20N30N40N50N60N70N80N

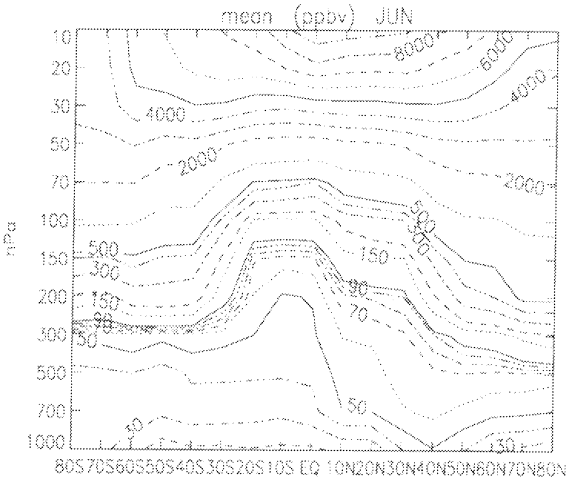
mean (ppbv) JUN
hPa
80S70S60S50S40S30S20S10S EQ 10N20N30N40N50N60N70N80N

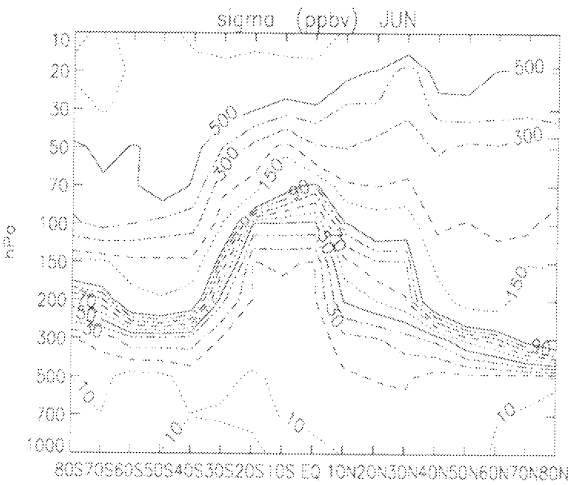
sigma (ppbv) JUN
hPa
80S70S60S50S40S30S20S10S EQ 10N20N30N40N50N60N70N80N

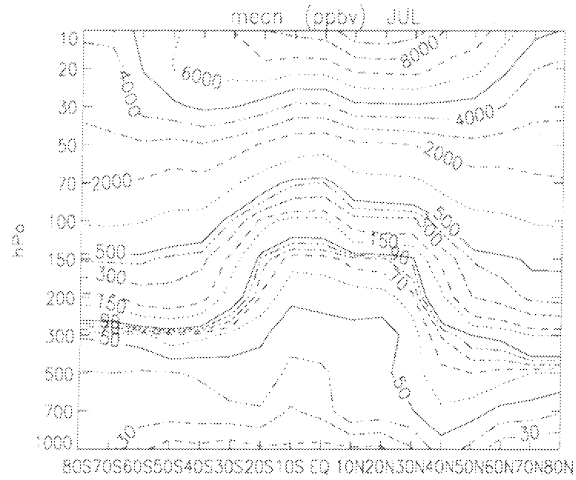
mean (ppbv) JUL
hPa
80S70S60S50S40S30S20S10S EQ 10N20N30N40N50N60N70N80N

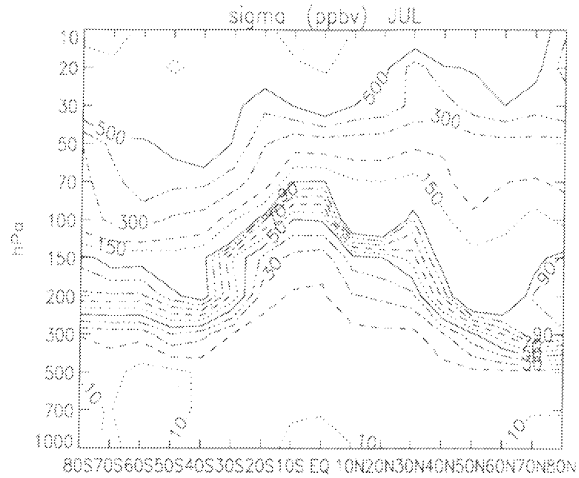
sigma (ppbv) JUL
hPa
80S70S60S50S40S30S20S10S EQ 10N20N30N40N50N60N70N80N

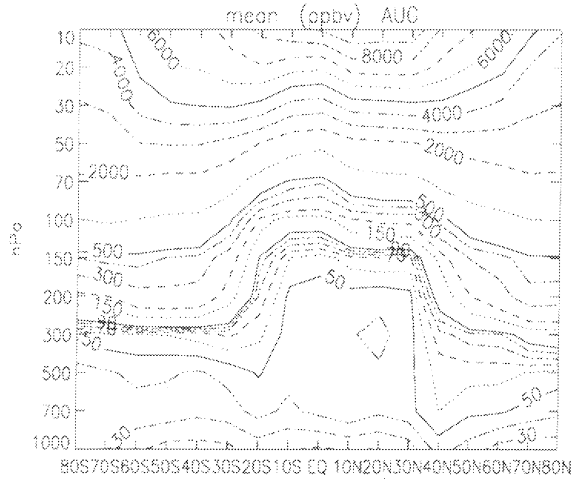
mean (ppbv) AUG
hPa
80S70S60S50S40S30S20S10S EQ 10N20N30N40N50N60N70N80N

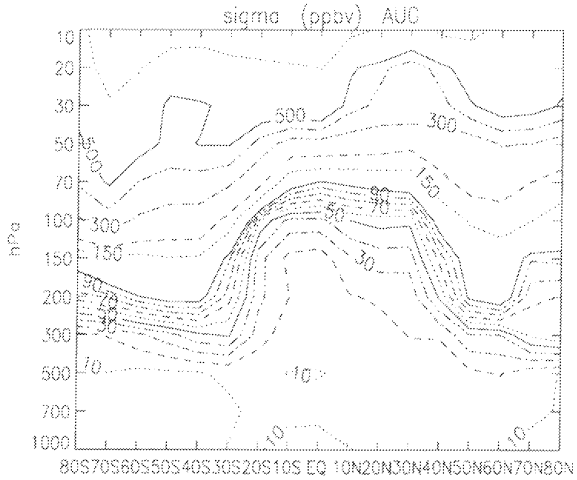
sigma (ppbv) AUG
hPa
80S70S60S50S40S30S20S10S EQ 10N20N30N40N50N60N70N80N

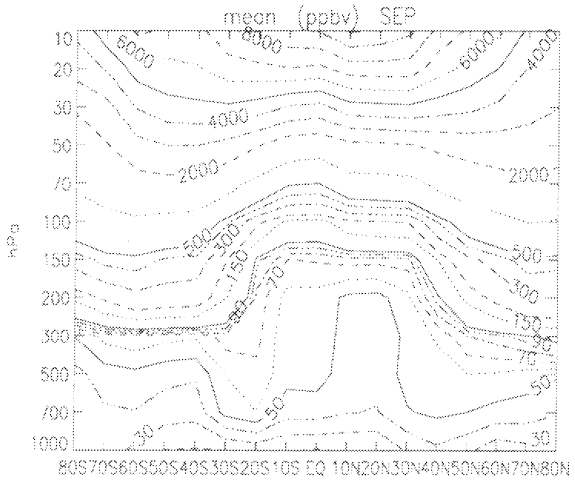
mean (ppbv) SEP
hPa
80S70S60S50S40S30S20S10S EQ 10N20N30N40N50N60N70N80N

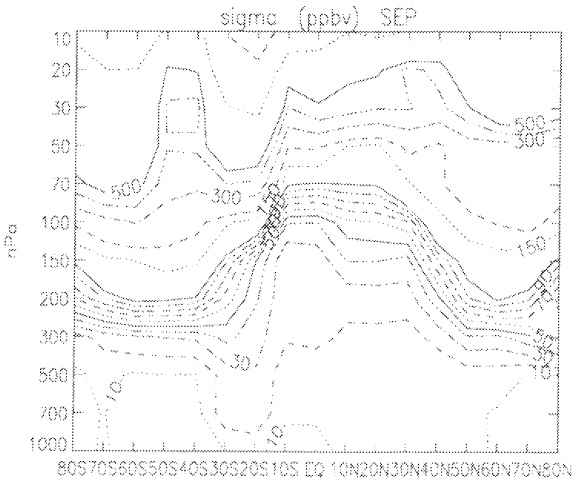
sigma (ppbv) SEP
hPa
80S70S60S50S40S30S20S10S EQ 10N20N30N40N50N60N70N80N

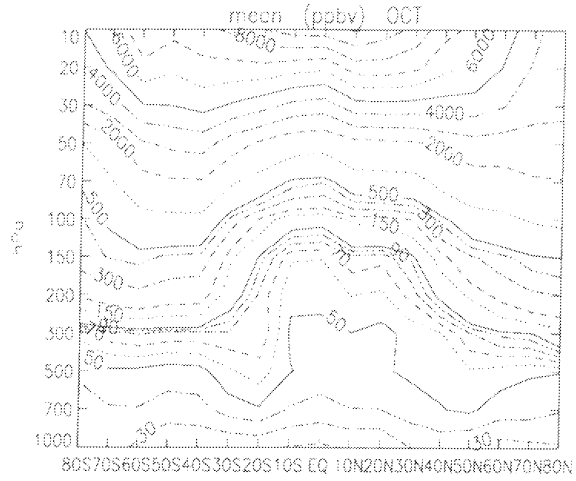
mean (ppbv) OCT
hPa
80S70S60S50S40S30S20S10S EQ 10N20N30N40N50N60N70N80N

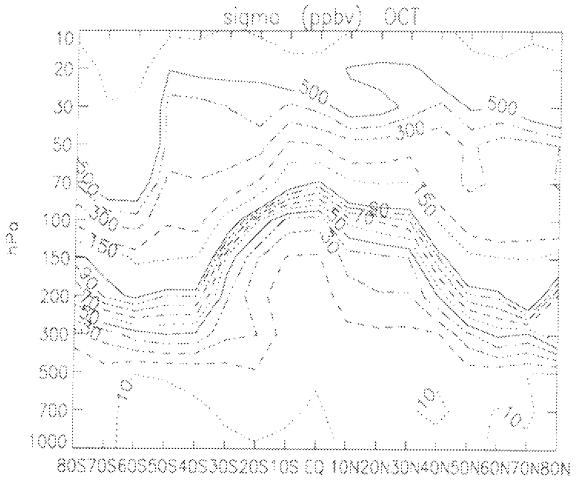
sigma (ppbv) OCT
hPa
80S70S60S50S40S30S20S10S EQ 10N20N30N40N50N60N70N80N

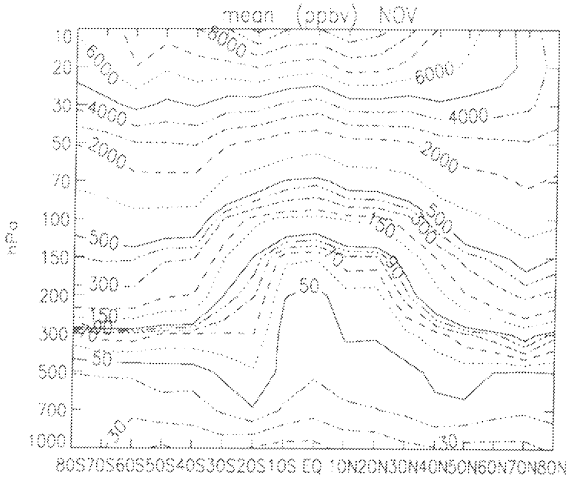
mean (ppbv) NOV
hPa
80S70S60S50S40S30S20S10S EQ 10N20N30N40N50N60N70N80N

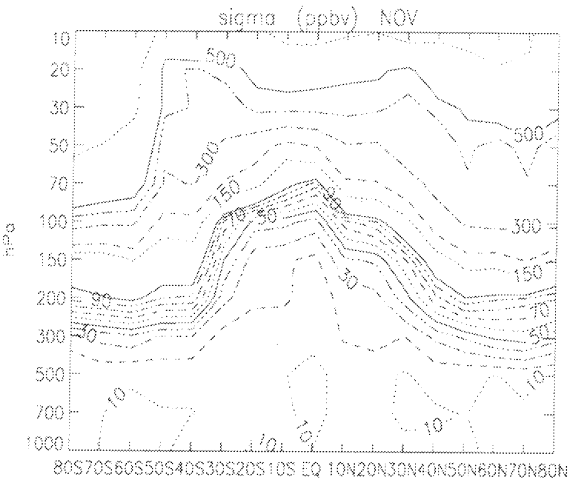
sigma (ppbv) NOV
hPa
80S70S60S50S40S30S20S10S EQ 10N20N30N40N50N60N70N80N

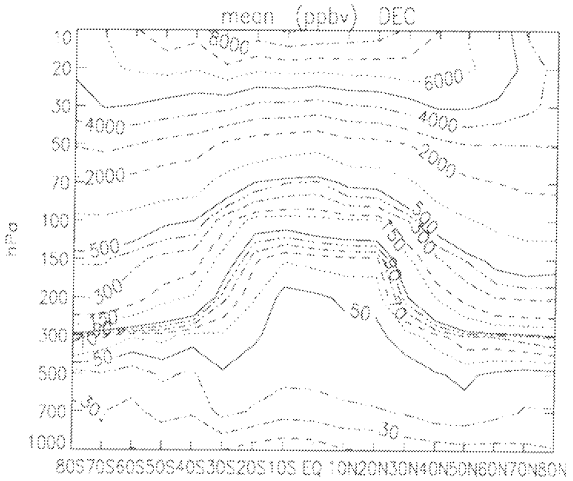
mean (ppbv) DEC
hPa
80S70S60S50S40S30S20S10S EQ 10N20N30N40N50N60N70N80N

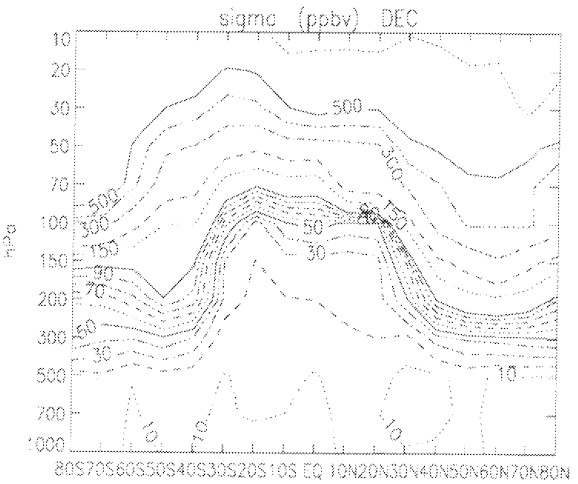
sigma (ppbv) DEC
hPa
80S70S60S50S40S30S20S10S EQ 10N20N30N40N50N60N70N80N

Acknowledgements

It is a pleasure for the author to thank those who contributed to the collection of stations used in this climatology. The Natal sonde data, which is the result of an international cooperation programme between the Instituto Nacional de Pesquisas Espacials (INPE) in Brazil and NASA in the USA, was provided by J. Logan, with the help of Y. Sahai and V.W.J.H. Kirchoff. Ozonesonde data for Samoa, Hilo, Boulder, and South Pole were given by S. Oltmans of the NOAA Climate Monitoring and Diagnostics Laboratory. The Reunion data comes from M. Bessafi and F. Taupin from the Laboratoire de Physique de l'Atmosphere in France. All the other ozonesonde data were retrieved from the World Ozone and Ultraviolet radiation Data Centre (WOUDC), courtesy of the Environment Canada/World Meteorological Organisation. E. Hare is especially acknowledged for his help in many matters related to the WOUDC data. The research was funded by the EC under the SINDICATE II (Study of INdirect and Direct Influences on Climate of Anthropogenic Trace gas Emissions, II) project number ENV4-CT95-090.

References

Andreae, M.O.: "Climatic effects of changing atmospheric aerosol levels" in *World Survey of Climatology, Volume 16: Future climates of the world*", A. Henderson-Sellers (Ed.), Elsevier Amsterdam (1994).

Andreae, M.O., J. Fishman, J.G. Goldhammer, C.O. Justice, J.S. Levine, R.J. Scholes, B.J. Stocks, A.M. Thompson, B. van Wilgen, and the STARE/TRACE-A/SAFARI Science team: "Biomass burning in the global Environment: First results from the IGAC/BIBEX field campaign STARE/TRACE-A/SAFARI-92" in *Global Atmospheric-Biospheric Chemistry*, R.G. Prinn (Ed.), Plenum, New York (1994).

Fishman, J., V.G. Brakett and K. Fakhruzzaman: "Distribution of tropospheric ozone in the tropics from satellite and ozonesonde measurements" *J. Atm. Terr. Phys.* **54**, p. 589-597 (1992).

Fortuin, J.P.F. and U. Langematz: "An Update on the Global Ozone Climatology and on Concurrent Ozone and Temperature Trends" in *Atmospheric Sensing and Modeling*, R.P. Santer (Ed.) Proc. SPIE 2311 Washington, DC, p.207-216 (1994).

Fortuin, J.P.F., R. van Dorland, W.M.F. Wauben and H. Kelder: "Greenhouse Effects of Aircraft Emissions as Calculated by a Radiative Transfer Model" *Ann. Geophys.* **13**, p. 413-418 (1995).

Keating, G.M, L.S. Chiou and N.C. Hsu: "Improved ozone reference models for the COSPAR International Reference Atmosphere" in *COSPAR International Reference Atmosphere (CIRA) Part III: Trace constituents reference models*, G.M. Keating (Ed.), Volume 18 number 9/10, Elsevier Science, UK (1996).

Kirchoff, V.W.J.H., R.A. Barnes and A.L. Torres: "Ozone climatology at Natal, Brazil, from in situ ozonesonde data" *J. Geophys. Res.* **96**, p. 10,899-10,909 (1991).

Logan, J.A.: "Tropospheric ozone: seasonal behaviour, trends, and anthropogenic influence" *J. Geophys. Res.* **90**, p. 10,463-10,482 (1985).

London, J., R.D. Bojkov, S. Oltmans and J.I. Kelley: "Atlas of the global distribution of total ozone, July 1957-June 1967" in *NCAR techn. note no. 113+STR*, Boulder Colorado (1976).

Wilcox, R.W., G.D. Nastrom and A.D. Belmont: "Periodic variations of total ozone and its vertical distribution" *J. Appl. Met.* **16**, p. 290-298 (1977).

KNMI-Publicaties, Technische & Wetenschappelijke Rapporten gepubliceerd sedert 1988

Een overzicht van alle publicaties van het Koninklijk Nederlands Meteorologisch Instituut die tussen 1849 en 1988 werden uitgegeven, wordt u op verzoek toegezonden door de Bibliotheek van het KNMI, postbus 201, 3730 AE De Bilt, tel. 030 - 2 206 855, fax. 030 - 2 210 407.

KNMI-publicatie met nummer

150-27	Normalen en extreme waarden van 15 hoofdstations voor het tijdvak 1961-90 / samenst. H.J. Krijnen ...[et al.]	1992
165-5	Historische weerkundige waarnemingen: beschrijving antieke meetreeksen / H.A.M. Geurts en A.F.V. van Engelen	1992
172	Vliegen in weer en wind: geschiedenis van de luchtvaartmeteorologie / Tj. Langerveld	1988
173	Werkdocument verspreidingsmodellen / red. H. van Dop ; in samenwerking met het RIVM	1988
174	Ons klimaat, onze planeet / voorw. H. Tennekes ; inleiding C.J.E. Schuurmans ; met bijdr. van H. van Dop ...[et al.]	1989
175	Klimaat-onderzoek Westland ten behoeve van kustuitbreiding / W.H. Slob	1989
176	Stormenkalender: chronologisch overzicht van alle stormen langs de Nederlandse kust 1964-1990 / B. Augustijn, H. Daan ...[et al.]	1990
177	Description of the RIVM-KNMI PUFF dispersion model / G.H.L. Verver ...[et al.]	1990
178	Modules A & B / Bureau Vorming en Opleiding **[uitsluitend intern beschikbaar]**	1991-
179	Catalogus van aardbevingen in Nederland / G. Houtgast	1991
179a	Catalogus van aardbevingen in Nederland : 2e, gewijzigde druk / G. Houtgast	1992
180	List of acronyms in environmental sciences / [P. Geerders]	1991
180a	List of acronyms in environmental sciences : revised edition / [P. Geerders and M. Waterborg]	1995
181	Nationaal gebruik van de groepen 7wwW1W2 en 960ww voor landstations / [samenst. H. van Drongelen ea.]	1992
181a	FM12 Synop : internationale en nationale regelgeving voor het coderen van de groepen 7wwW1W2 en 960ww	1995
181b	FM12 Synop : internationale en nationale regelgeving voor het coderen van de groepen 7wwW1W2 en 960ww ; derde herziene versie	1996
182	Wijziging aeronautische codes : 1 juli 1993 / [P.Y. de Vries en A.A. Brouwer]	1993
183-1	Rainfall in New Guinea (Irian Jaya) / T.B. Ridder	1995
183-2	Vergelijking van zware regens te Hollandia (Nieuw Guinea), thans Jayapura (Irian Jaya) met zware regens te De Bilt / T.B. Ridder	1995
183-3	Verdamping in Nieuw-Guinea, vergelijking van gemeten hoeveelheden met berekende hoeveelheden / T.B. Ridder	1995
183-4	Beschrijving van het klimaat te Merauke, Nieuw Guinea (Irian Jaya) in verband met de eventuele vestiging van een zoutwinningsbedrijf aldaar / T.B. Ridder en H.W.H. Weeda	1995
183-5	Overzicht van klimatologische en geofysische publikaties betreffende Nieuw-Guinea / T.B. Ridder	1995
184	Inleiding tot de algemene meteorologie : studie-uitgave / B. Zwart, A. Steenhuisen, m.m.v. H.J. Krijnen	1994
184a	Inleiding tot de algemene meteorologie : studie uitgave ; 2e, geheel herziene druk / B. Zwart, A. Steenhuisen, m.m.v. H.J. Krijnen ea.	1995
185	Handleiding voor het gebruik van sectie 2 van de FM 13-X SHIP code door stations op zee / KNMI; Kon. Luchtmacht; Kon. Marine	1994
185a	Handleiding voor het gebruik van sectie 2 van de FM 13-X SHIP-code voor waarnemers op zee / KNMI; Kon.Luchtmacht, Kon.Marine	1995

Overigen

	Zonnestraling in Nederland / C.A. Velds (in samenwerking met uitgeverij Thieme in de serie "Het klimaat van Nederland"; 3)	1992

Technisch rapport = technical report (TR) - ISSN 0169-1708

103a	Wind-chill [geheel herziene versie] / B. Zwart	1992
105	Description of the Cabauw turbulence dataset 1977-1979 / C. Hofman	1988
106	Automatische detektie van inversies met sodar / A.C.M. Beljaars en R. Agterberg	1988
107	Numerieke atmosfeermodellen / A.P.M. Baede	1988
108	Inpassing van Meteosat informatie in de meteorologische besluitvorming / J. Roodenburg	1988
109	Opmeting van het aardmagneetveld in Nederland, herleid naar 1985 / J.H. Rietman	1988
111	Van Penman naar Makkink: een nieuwe berekeningswijze voor de klimatologische verdampingsgetallen / red. J.C. Hooghart ...[et al.]	1988
112	Description of a software library for the calculation of surface fluxes / A.C.M. Beljaars ...[et al.]	1989
113	Menghoogteberekeningen voor het Europees continent: een vergelijkend onderzoek / M.P. Scheele en H. van Dop	1989
114	Operational WAMS statistics over the period December 1986 - March 1987 / R.A. van Moerkerken ...[et al.]	1989
115	Mesoscale terrain roughness mapping of the Netherlands / R. Agterberg and J. Wieringa	1989
116	Geschiedenis van de landbouwmeteorologie in Nederland tot 1972 / J.P.M. Woudenberg	1989
117	Instabiliteiten rond de straalstroom / R.P. Henzen	1989
118	Verfificatie van de GONO golfverwachting over de periode oktober 1987 - april 1988 / R.A. van Moerkerken	1989
119	Spectra en gradienten van hoge windsnelheden te Cabauw tot 200 meter / R.W.M. Meijer	1989
120	About the possibilities of using an air transformation model in Tayun, Shanxi province, China / J. Reiff ...[et al.]	1989
121	The effect of wave data assimilation of the numerical simulation of wave energy advection / M. de las Heras ...[et al.]	1990
122	Objective analysis of precipitation observations during the Chernobyl episode / M.P. Scheele and G.H. Verver	1990
123	The use of satellite data in the ECMWF analysis system / K. Lablancz	1990
124	A primitive equation model for the Equatorial Pacific / M.A.F. Allaart and A. Kattenberg	1990
125	Technical description of the high-resolution air mass transformation model at KNMI / E.I.F. de Bruin ...[et al.]	1990
126	Verificatie kwantitatieve neerslagverwachting korte termijn (proefperiode) voor 5 regio's / D. Messerschmidt	1990
127	Quantitative processing of Meteosat-data: implementation at KNMI: applications / S.H. Muller	1990
128	A primary experiment of statistical interpolation schemes used in sea wave data assimilation / Gao Quanduo	1990
129	Coordinate conversions for presenting and compositing weather radar data / H.R.A. Wessels	1990
130	Flux-profile relationships in the nocturnal boundary layer / P. Bouwman	1990
131	The implementation of the WAQUA/CSM-16 model for real time storm surge forecasting / J.W. de Vries	1991
132	De luchttemperatuur boven West-Ameland / F. Ynsen	1991
133	Seizoenverloop en trend in de chemische samenstelling van de neerslag te Lelystad / T.A. Buishand en J.H. Baard	1991
134	Technical description of LAM and OI: Limited Area Model and Optimum Interpolation analysis / W.C. de Rooy ...[et al.]	1991
134a	Technical description of LAM and OI: Limited Area Model and Optimum Interpolation analysis, 2nd edition / W.C. de Rooy ...[et al.]	1992
135	Relatieve trajectorien in en rond een depressie / J.P.A.J. van Beeck	1991
136	Bepaling van een directe en diffuse straling en van zonneschijnduur uit 10-minuutwaarden van de globale straling / W.H. Slob ...[et al.]	1991

137	LAM en NEDWAM statistics over the period October 1990 - April 1991 / R.A. van Moerkerken	1991
138	Dagsom van de globale straling : een rekenmethode en verwachtingsverificatie / M.C. Nolet	1991
139	A real-time wave data quality control algorithm / Maria Paula Etala	1991
140	Syllabus Fysische Meteorologie I / H.R.A. Wessels	1991
141	Systeembeschrijving Mist Voorspel Systeem MIVOS / D. Blaauboer, H.R.A. Wessels en S. Kruizinga	1992
142	Het nachtelijk windmaximum : een interactieve verwachtingsmethode / N. Maat en H. Bakker	1992
143	Neerslagverificatie LAM / W.C. de Rooy en C. Engeldal	1992
144	Aanpassing vocht-bedekkingsgraadrelaties in het LAM / W.C. de Rooy	1992
145	Een verificatie van de Eurogids, de gidsverwachting voor vervoer en toerisme / H.G. Theihzen	1992
146	The earth radiation budget experiment : overview of data-processing and error sources / Arnout J. Feijt	1992
147	On the construction of a regional atmospheric climate model / Jens H. Christensen and Erik van Meijgaard	1992
148	Analyse van torenwindgegevens over het tijdvak 1977 tot en met 1991 / Gertie Geertsema	1992
149	The performance of drag relations in the WAQUA storm surge model / J.R.N. Onvlee	1993
150	Verifications of 3I retrievals vis-à-vis radiosonde observations / G.J. Prangsma	1993
151	Het Synoptusch Symposium : een verslag / red. H.G. Theihzen	1993
152	The ACIFORN hydrological programme : the water cycle of a Douglas fir forest / F.C. Bosveld ...[et al.]	1993
153	Het APL+-prgramma / R.M. van Westrhenen	1993
154	The effect of spatial averaing on threshold exceedances of daily precipitation amounts / T.A. Buishand,	1993
155	Neerslagvergelijking van Espelo ten opzichte van het omgevingsgemiddelde / J.P.M. van Dun en J. Verloop	1993
156	On the effects of limited spectral resolution in third-generation wave models / I.V. Lavrenov and J.R.A. Onvlee	1993
157	Meteorologische evaluatie van de zichtmetingen langs de A16 / H.R.A. Wessels	1993
158	Het programma voor berekening van zonneschijnduur uit globale straling / U. Bergman	1993
159	Verificatie weersverwachtingen 1955 - 1993 / H. Daan	1993
160	Drie objectieve indices voor clear-air turbulence nader bekeken / H. Bakker	1993
161	The ASGASEX experiment / W.A. Oost	1994
162	TEBEX observations of clouds and radiation -potential and limitations / P. Stammes ...[et al.]	1994
163	Evaluatie kwaliteitsonderzoek mistdata "Mistprojekt A-16" Breda / M. van Berchum	1994
164	Standaard stralingsmetingen met een zonnevolger / A.C.A.P. van Lammeren en A. Hulshof	1994
165	Neurale netwerken versus lineaire regressie / R.M. Meuleman	1994
166	Seismische analyse van de aardbeving bij Alkmaar op 6 augustus 1994 / [SO]	1994
167	Seismische analyse van de aardbeving bij Alkmaar op 21 september 1994 / [SO]	1994
168	Analyse van het seismische risico in Noord-Nederland / Th. de Crook, B. Dost en H.W. Haak	1995
169	Evaluatie van neerslagprognoses van numerieke modellen voor de Belgische Ardennen in december 1993 / Erik van Meijgaard	1994
170	DARR-94 / C.P.G. Lomme	1994
171	EFEDA-91 : documentation of measurements obtained by KNMI / W.A.A. Monna ...[et al.]	1994
172	Cloud lidar research at the Royal Netherlands Meteorological Institute and KNMI2B2 version 2 cloud lidar analysis software documentation / Alexandre Y. Fong and André C.A.P. van Lammeren	1994
173	Measurements of the structure parameter of vertical wind-velocity in the atmospheric boundary layer / R. van der Ploeg	1995
174	Report of the ASGASEX'94 workshop / ed. by W.A. Oost	1995
175	Over slecht zicht, bewolking, windstoten en gladheid / J. Terpstra	1995
176	Verification of the WAQUA/CSM-16 model for the winters 1992-93 and 1993-94 / J.W. de Vries	1995
177	Nauwkeuriger nettostraling meten / M.K. van der Molen en W. Kohsiek	1995
178	Neerslag in het stroomgebied van de Maas in januari 1995: waarnemingen en verificatie van modelprognoses / Rudmer Jilderda ...[et al.]	1995
179	First field experience with 600PA phased array sodar / Henk Klein Baltink	1995
180	Een Kalman-correctieschema voor de wegdektemperatuurverwachtingen van het VAISALA-model / A. Jacobs	1995
181	Calibration study of the K-Gill propeller vane / Marcel Bottema	1995
182	Ontwikkeling van een spectraal UV-meetinstrument / Frank Helderman	1995
183	Rainfall generator for the Rhine catchment : a feasibility study / T. Adri Buishand and Theo Brandsma	1996
184	Parametrisatie van mooi-weer cumulus / M.C. van Zanten	1995
185	Interim report on the KNMI contributions to the second phase of the AERO-project / Wiel Wauben, Paul Fortuin ...[et al.]	1995
186	Seismische analyse van de aardbevingen bij Middelstum (30 juli 1994) en Annen (16 augustus 1994 en 31 januari 1995) / [SO]	1995
187	Analyse wenselijkheid overname RIVM-windmeetlokaties door KNMI / H. Benschop	1996
188	Windsnelheidsmetingen op zeestations en kuststations: herleiding waarden windsnelheden naar 10-meter niveau / H. Benschop	1996
189	On the KNMI calibration of net radiometers / W. Kohsiek	1996
190	NEDWAM statistics over the period October 1994 - April 1995 / F.B. Koek	1996
191	Description and verification of the HIRLAM trajectory model / E.I.F. de Bruijn	1996
192	Tiltmeting : een alternatief voor waterpassing ? / H.W. Haak	1996
193	Error modelling of scatterometer, in-situ and ECMWF model winds; a calibration refinement / Ad Stoffelen	1996

Wetenschappelijk rapport = scientific report (WR) - ISSN 0169-1651

88-01	Central Sudan surface wind data and climate characteristics / E.H. ABu Bakr
88-02	Startocumulus modeling / P.G. Duynkerke
88-03	Naar een niet-linear wateropzetmodel : stand van zaken februari 1988 / C.J. Kok
88-04	The boundary layer wind regime of a representative tropical African region, central Sudan / E.H. ABu Bakr
88-05	Radiative cooling in the nocturnal boundary layer / S.A. Tjemkes
88-06	Surface flux parameterization schemes : developments and experiences at KNMI / A.A.M. Holtslag and A.C.M. Beljaars
89-01	Instability mechanisms in a barotropic atmsophere / R.J. Haarsma
89-02	Climatological data for the North Sea based on observations by volutary observing ships over the period 1961-1980 / C.G. Korevaar
89-03	Verificatie van GONO golfverwachtingen en van Engelse fine-mesh winden over de periode oktober 1986 - april 1987 / R.A. van Moerkerken
89-04	Diagnostics derivation of boundary layer parameters from the outputs of atmospheric models / A.A.M. Holtslag ...[et al.]
89-05	Statistical forecasts of sushine duration / Li Zhihong and S. Kruizinga
90-01	The effect of a doubling atmospheric CO2 on the stormtracks in the climate of a GCM / P.C. Siegmund
90-02	Analysis of regional differences of forecasts with the multi-layer AMT-model in the Netherlands / E.I.F. de Bruin, Li Tao Guang ...[et al.]
90-03	Description of the CRAU- data-set: Meteosat data, radiosonde data, sea surface temperatures : comparison of Meteosat and Heimann-data / S.H. Muller, H. The, W. Kohsiek and W.A.A. Monna
90-04	A guide to the NEDWAM wave model / G. Burgers
91-01	A parametrization of the convective atmospheric boundary layer and its application into a global climate model / A.A.M. Holtslag ...[et al.]

91-02 Turbulent exchange coefficients over a Douglas fir forest / F.C. Bosveld
92-01 Experimental evaluation of an arrival time difference lightning positioning system / H.R.A. Wessels
92-02 GCM control run of UK Met.Office compared with the real climate in the Northwest European winter / J.J. Beersma
92-03 The parameterization of vertical turbulent mixing processes in a General Circulation Model of the Tropical Pacific / G. Janssen
92-04 A scintilation experiment over a forest / W. Kohsiek
92-05 Grondtemperaturen / P.C.T. van der Hoeven en W.N. Lablans
92-06 Automatic supression of anomalous propagation clutter for noncoherent weather radars / H.R.A. Wessels ...[et al.]
93-01 Searching for stationary stable solutions of Euler's equation / R. Salden
93-02 Modelling daily precipitation as a function of temperature for climatic change impact studies / A.M.G. Klein Tank and T.A. Buishand
93-03 An analytical conceptual model of extratropical cyclones / L.C. Heijboer
93-04 A synoptic climatology of convective weather in the Netherlands / Dong Hongnian
93-05 Conceptual models of severe convective weather in the Netherlands / Dong Hongnian
94-01 Seismische analyse van aardbevingen in Noord-Nederland : bijdrage aan het multidisciplinaire onderzoek naar de relatie tussen gaswinning en aardbevingen / H.W. Haak en Th. de Crook
94-02 Storm activity over the North Sea and the Netherlands in two climate models compared with observations / J.J. Beersma
94-03 Atmospheric effects of high-flying subsonic aircraft / W. Fransen
94-04 Cloud-radiation-hydrological interactions : measuring and modeling / A. Feijt ...[et al.]
94-05 Spectral ultraviolet radiation measurements and correlation with atmospheric parameters / F. Kuik and H. Kelder
95-01 Transformation of precipitation time series for climate change impact studies / A.M.G. Klein Tank and T.A. Buishand
95-02 Internal variability of the ocean generated by a stochastic forcing / M.H.B. van Noordenburg
95-03 Applicability of weakly nonlinear theory for the planetary-scale flow / E.A. Kartashova
95-04 Changes in tropospheric NOx and O3 due to subsonic aircraft emissions / W.M.F. Wauben ...[et al.]
95-05 Numerical studies on the Lorenz-84 atmosphere model / Leonardo Anastassiades
95-06 Regionalisation of meteorological parameters / W.C. de Rooy
95-07 Validation of the surface parametrization of HIRLAM using surface-based measurements and remote sensing data / A.F. Moene, H.A.R. de Bruin ...[et al.]
95-08 Probabilities of climatic change : a pilot study / Wieger Fransen (ed.) and Alice Reuvekamp
96-01 A new algorithm for total ozone retrieval from direct sun measurements with a filter instrument / W.M.F. Wauben
96-02 Chaos and coupling: a coupled atmosphere ocean-boxmodel for coupled behaviour studies / G. Zondervan
96-03 An acoustical array for subsonic signals / H.W. Haak
96-04 Transformation of wind in the coastal zone / V.N. Kudryavtsev and V.K. Makin
96-05 Simulations of the response of the ocean waves in the North Atlantic and North Sea to CO2 doubling in the atmosphere / Kathy M. Rider ...[et al.]
96-06 Microbarograph systems for the infrasonic detection of nuclear explosions / H.W. Haak and G.J. de Wilde
96-07 An ozone climatology based on ozonesonde measurements / J.P.F. Fortuin